Statistical Field Estimation for Complex Coastal Regions and Archipelagos☆

First A. Author[a], Second B. Author, Jr.[b]

Massachusetts Institute of Technology, Cambridge, MA-02139, USA

[a] *e-mail: author@mit.edu*
[b] *e-mail: author@mit.edu*

Abstract

A fundamental requirement in realistic computational geophysical fluid dynamics is the optimal estimation of gridded fields directly from the spatially irregular and multivariate data sets that are collected by varied instruments and sampling schemes. In this work, we derive and utilize new schemes for the mapping and dynamical inference of ocean fields in complex multiply-connected domains and study the computational properties of our new mapping schemes. Objective Analysis (OA) is the statistical estimation of fields using the Bayesian-based Gauss-Markov theorem, i.e. the update step of the Kalman Filter. The existing multi-scale OA approach of the Multidisciplinary Simulation, Estimation and Assimilation System consists of the successive utilization of Kalman update steps, one for each scale and for each correlation across scales. In the present work, the approach is extended to field mapping in complex, multiply-connected, coastal regions and archipelagos. A reasonably accurate correlation function often requires an estimate of the distance between data and model points, without going across complex landforms. New methods for OA based on estimating the length of optimal shortest sea paths using the Level Set Method (LSM) and Fast Marching Method (FMM) are derived, implemented and utilized in general idealized and realistic ocean cases. Our new methodologies could improve widely-used gridded databases such as the climatological gridded fields of the World Ocean Atlas (WOA) since these oceanic maps were computed without accounting for the

☆We are grateful to the Office of Naval Research for research support under grants N00014-07-1-1061 and N00014-08-1-1097 (ONR6.1), N00014-07-1-0473 (PhilEx) and S05-06 (PLUSNet) to the Massachusetts Institute of Technology.

coastline constraints. A new FMM-based methodology for the estimation of absolute velocity under geostrophic balance in complicated domains is also discussed. Our new schemes are compared with other approaches, including the use of stochastically forced partial differential equations (SPDE). We find that our FMM-based scheme for complex, multiply-connected, coastal regions is more efficient and accurate than the SPDE approach. We also show that the field maps obtained using our FMM-based scheme do not require postprocessing (smoothing) of fields. The computational properties of our new mapping schemes are studied in detail. We find that higher-order schemes improve the accuracy of distance estimates. We also show that the covariance matrices we estimate are not necessarily positive definite because the Weiner Khinchin and Bochner relationships for positive definiteness are only valid for convex simply-connected domains. Several approaches to overcome this issue are discussed and qualitatively evaluated. The solutions we propose include introducing a small process noise or reducing the covariance matrix based on the dominant singular value decomposition.

Key words:
Field Mapping, Objective Analysis, Levitus Climatology, Fast Marching Method, Level Set Method, Gauss-Markov Estimation, Geostrophy

---

1. Introduction and Motivation

The statistical estimation theory of Objective Analysis (OA) was introduced by Gandin (1965) to the field of meteorology and was extended to oceanography by Bretherton et al. (1976). The theory is based on the Gauss-Markov theorem (Plackett, 1950), and it provides a sound basis for interpolating irregularly spaced data onto a computational grid. Upto details of the set-up, which are specific to the oceanic and atmospheric fields, the OA scheme is equivalent to utilize the Kalman update steps of the Kalman Filter to grid the irregularly-spaced data. Specifically, the data is gridded based on the specified prior field estimate and error covariance matrices. The OA methodology has been well formulated for open oceans without any landforms (convex simply-connected domains), but the OA in complex coastal regions (multiply-connected domains) is one of the 'last' mapping problems which remains to be studied in detail. This is one of the main research question of the present work.

Our OA research is carried out within the Multidisciplinary Simulation,

Estimation and Assimilation System (MSEAS: http://mseas.mit.edu) group. MSEAS consists of a set of mathematical models and computational methods for ocean predictions and dynamical diagnostics, for optimization and control of autonomous ocean observation systems, and for data assimilation and data-model comparisons. It is used for basic and fundamental research and for realistic simulations and predictions in varied regions of the world's ocean, recently including monitoring (Lermusiaux, 2007), naval exercises including real-time acoustic-ocean predictions (Xu et al., 2008) and environmental management (Cossarini et al., 2009). Several different models are included in the MSEAS, including a new free-surface primitive-equation dynamical model which uses two-way nesting free-surface and open boundary condition schemes (Haley et al., 2008). This new free-surface code is based on the primitive-equation model of the Harvard Ocean Prediction System (HOPS). Additionally, barotropic tides are calculated from an inverse tidal model (Logoutov, 2008).

In MSEAS, the Kalman updates for data gridding are carried out successively, from the largest scale (uniform mean prior) to the smallest scale, using a sequential processing of observations and scale separation. In a two-scale version, a two-staged OA approach (Lermusiaux, 1997, 1999) maps the scarcely available data onto oceanic fields in two steps: the larger and the smaller scale steps. The two main requirements for the Objective Analysis based on a Kalman update (also called the Gauss Markov estimation theory) are the statistical description of the field being estimated and the observational noise covariance. While observational noise statistics is dependent on the measurement sensor, the knowledge of the field statistics does not come easily in oceanography due to the scarcity of observations. A description of field statistics is often provided by a simple analytical correlation function which depends on the spatial separation distance and the spatial-temporal scales (Carter and Robinson, 1987). Other schemes also utilize dynamical models to construct covariances.

Our research study on Objective Analysis for coastal regions has been motivated by the Philippines Straits Dynamics Experiment (PhilEx) sponsored by the Office of Naval Research. The goal of PhilEx is to enhance understanding of the oceanographic processes and features arising in and around straits, and to improve the capability to predict the inherent spatial and temporal variability of these regions using models and advanced data assimilation techniques. There are several examples of Objective Analysis in coastal regions (Hessler, 1984; Stacey et al., 1988; Paris et al., 2002), but

the methodologies employed in these examples do not satisfy the coastline constraints (e.g. there should be no direct relationship across landforms).

New methodologies for field (e.g. temperature, salinity, biology, and velocity) mapping in complex multiply-connected coastal domains and archipelagos are derived and demonstrated in this paper. These methodologies will likely be very useful in improving the World Ocean Atlas (WOA) climatologies in complex multiply-connected domains. The WOA provides global ocean climatology containing monthly, seasonal and annual means of temperature (T) and salinity (S) fields at standard ocean depths. The temperature and salinity climatologies presented as part of the WOA (Levitus, 1982), which is also termed as 'Levitus Climatology' and its atlas updates in 1994 (Levitus and Boyer, 1994; Levitus et al., 1994), 1998 (Antonov et al., 1998a,b,c; Boyer et al., 1998a,b,c), 2001 (Stephens et al., 2002; Boyer et al., 2002) and 2005 (Locarnini et al., 2006; Antonov et al., 2006; Garcia et al., 2006a,b) have proven to be valuable tools for studying the hydrographic structures of the World's oceans. The WOA climatologies have been very useful for providing initial and boundary conditions to ocean circulation models. As its MSEAS counterpart, the OA procedure for 'Levitus Climatology' requires the use of an analytical correlation function to determine the covariance (or weight function, as described by Levitus (1982)). If the "straight Euclidean distance" (the straight line distance between two points) is used in such analytical correlation functions, the distance estimate is inappropriate for complex multiply-connected domains, as this "straight Euclidean distance" goes across land and so violate the coastline constraints. The aim of the new methodologies proposed in this paper is to satisfy the coastline constraints in complex multiply-connected domains.

The paper is organized as follows: The problems addressed in this paper are described in Section 2. In Section 3, we review the two staged multiscale static field mapping approach from MSEAS. In Section 4, we introduce the new OA methodologies based on the Level Set Method and the Fast Marching Method. An optimization approach for computing the transport streamfunction and absolute velocity under geostrophic balance by minimizing the inter-island transport is also discussed. The OA approach based on the stochastically forced partial differential equations (SPDE) is introduced in Section 5. In Section 6, applications of our new methodologies, for the complex regions of Dabob Bay and Philippines Archipelago are presented. In Section 7, we study the computational properties of our new mapping schemes. Section 8 consists of a summary and conclusions.

2. Problem Statement

We begin by introducing the definitions of convex domains, simply and multiply connected domains. A domain is said to be convex if for every pair of points within the domain, every point on the straight line segment that joins them is also within the domain. A domain is said to be simply-connected if any closed curve within it can be continuously shrunk to a point without leaving the domain. A domain which is not simply-connected is called multiply-connected.

The main research question of this work is field mapping in complex multiply-connected coastal domains. As discussed in Section 1, this is one of the 'last' mapping problems which remains to be studied in detail. Objective Analysis requires a description of field statistics which is often provided by analytical correlation functions (Carter and Robinson, 1987). Such analytical correlation functions are dependent on the spatial separation distance. We have also discussed in Section 1 that the use of "straight Euclidean distance" in complex multiply-connected domains is not appropriate since there is no direct relationship across landforms. An appropriate measure of distance to be used in the correlation function for OA in such complex multiply-connected regions should be longer. It is nonetheless the length of the optimal shortest sea path i.e., the shortest path without going across complex landforms. Examples of the optimal path length in sub-domains of Monterey Bay, Massachusetts Bay, Dabob Bay and Philippines Archipelago are illustrated in Figure 1. Here, we have considered the optimal shortest sea path, but in future we would like to investigate the selection of paths which governs the dynamics in the ocean.

Such an optimal shortest sea path in complex multiply-connected regions can be obtained using the following numerical techniques: the Level set method (LSM) (Osher and Sethian, 1988; Sethian, 1999b) and the Fast Marching Method (FMM) (Sethian, 1996, 1999b). These methods model the propagation of evolving boundaries using appropriate PDE's. They have been applied in both the Philippines Archipelago and Dabob Bay (WA, USA) regions. Other optimization methods for path planning, for example Dijkstra's algorithm (Bertsimas and Tsitsiklis, 1997) and Bresenham-based line algorithm (Bresenham, 1965) could also be used for mapping in complex domains, but FMM and LSM schemes are shown to be computationally more efficient and more accurate. These methods are also compared to the OA approach based on using the stochastically forced partial differential equations

(Balgovind et al., 1983; Lynch and McGillicuddy, 2001).

The FMM and LSM can also be utilized for estimating the minimum vertical area along any path between two islands. Vertical areas across landforms are needed to compute the transport streamfunction along the island coastlines, which minimizes the inter island transport. Such estimates of the transport streamfunction will aid in the computation of absolute velocity under geostrophic balance (Wunsch, 1996) in complex domains with islands.

Computational properties of the new mapping schemes are also investigated in detail. To reduce the computational cost and to understand the impact of individual data, sequential processing of observations (Parrish and Cohn, 1985; Cho et al., 1996) is utilized. By definition, the prior covariance matrix should be positive definite. According to the Wiener-Khinchin and Bochner theorem (Papoulis, 1991; Yaglom, 2004; Dolloff et al., 2006), the covariance matrix based on analytical correlation function will be positive definite if the Fourier transform (or the spectral density of the correlation function) is non-negative for all frequencies. These theorems are valid only for convex simply-connected domains. In our complex multiply-connected domains, the covariance matrix may become negative due to: a. Numerical error in the computation of the optimal path length using our new FMM/LSM based schemes b. The presence of landforms. These issues may lead to divergence problems (Brown and Hwang, 1997) in the field mapping schemes. Therefore, the following two questions were resolved and investigated: a). What are the computational errors in optimal path lengths computed using the FMM/LSM and how can they be reduced? b). What are the computational issues including non-positive definite covariances that arise in a multiply-connected coastal domain and how can they be remedied? These computational studies were indispensable for the development of our novel FMM/LSM based scheme for complex multiply-connected domains.

3. MSEAS Objective Analysis Approach

The multi-scale OA approach from MSEAS, which require the computation of Euclidean distance, is well established for mapping heterogeneous, multivariate, irregular data (Gandin, 1965; Bretherton et al., 1976; Carter and Robinson, 1987; Daley, 1993) in open oceans without islands or archipelagos as well as in atmospheric sciences. The two staged OA approach (Lermusiaux, 1997, 1999) in MSEAS, utilizes the Gauss-Markov or minimum error variance criterion (Plackett, 1950) to map observations to the numerical grid.

Let us denote the vector of numerical grid point locations as $\mathbf{x}$ and the vector of measurement locations as $\mathbf{X}$, then the OA estimate of the field ($\psi^{\mathbf{OA}}$) based on the background field ($\bar{\psi}$,$\bar{\mathbf{d}}$) is given by:

$$\begin{aligned} \psi^{\mathbf{OA}} &= \bar{\psi} + Cor(\mathbf{x},\mathbf{X})[Cor(\mathbf{X},\mathbf{X}) + \mathbf{R}]^{-1}[\mathbf{d} - \bar{\mathbf{d}}] \\ &= \bar{\psi} + \mathbf{K}[\mathbf{d} - \bar{\mathbf{d}}] \end{aligned} \tag{1}$$

where, $\bar{\mathbf{d}} = \mathbf{H}\bar{\psi}$, $\mathbf{H}$ is the observation matrix, $\mathbf{d}$ is the sensor data vector, $\mathbf{R}$ is the observational error covariance matrix, and Gain ($\mathbf{K}$) is given by:

$$\mathbf{K} = Cor(\mathbf{x},\mathbf{X})[Cor(\mathbf{X},\mathbf{X}) + \mathbf{R}]^{-1} \tag{2}$$

The error covariance of the estimated field is given by:

$$\begin{aligned} \mathbf{P}^{\mathbf{OA}} &= E[(\mathbf{x} - E[\mathbf{x}])(\mathbf{x} - E[\mathbf{x}])^T] \\ &= Cor(\mathbf{x},\mathbf{x}) - \mathbf{K}Cor(\mathbf{X},\mathbf{x}). \end{aligned} \tag{3}$$

A comparison between the MSEAS update equations (OA) and the Kalman filter (KF) update equations is made in Table 1.

KF Update Equations	MSEAS Update equations
Kalman gain: $\mathrm{K_t = P_{t\|t-1} H_t^T \times [H_t P_{t\|t-1} H_t^T + R_t]^{-1}}$	OA estimator: Gain = Cor($\mathbf{x}$,$\mathbf{X}$)$\times[Cor(\mathbf{X},\mathbf{X}) + \mathbf{R}]^{-1}$
State estimate update: $\hat{x}_t = \hat{x}_{t\|t-1} + K_t(y_t - H_t\hat{x}_{t\|t-1})$	State estimate update: $\psi^{OA} = \bar{\psi} + Gain[\mathbf{d} - \bar{\mathbf{d}}]$.
Error Covariance equation: $P_t = (I - K_t H_t)P_{t\|t-1}$	Error Covariance equation: $\mathbf{P}^{OA} = Cor(\mathbf{x},\mathbf{x}) - Gain \times Cor(\mathbf{X},\mathbf{x})$

Table 1: Comparison between the Kalman Filter and the MSEAS OA update equations.

Thus, the update equations of OA are equivalent to the update equations of the discrete Kalman filter algorithm where the background error correlation matrix for the field-to-data points, Cor($\mathbf{x}$,$\mathbf{X}$), and the background correlation matrix at the data points, Cor($\mathbf{X}$,$\mathbf{X}$), are directly related to the KF a priori error covariance matrix $P_{t|t-1}$ i.e. Cor($\mathbf{x}$,$\mathbf{X}$) = $P_{t|t-1}H_t^T$ and Cor($\mathbf{X}$,$\mathbf{X}$) = $H_t P_{t|t-1} H_t^T$ (H_t is the observation matrix). The matrix $\mathbf{R}$ represents the error covariance for the sensor data $\mathbf{d}$ at the data points. This matrix is

often chosen diagonal with a uniform non-dimensional error variance ϵ^2, i.e. $\mathbf{R} = \epsilon^2 I$. In MSEAS, the correlation matrices are often generated from the following isotropic function:

$$Cor(r) = \left(1 - \frac{r^2}{L_0^2}\right) exp\left[-0.5 \times (\frac{r^2}{L_e^2} + \frac{\Delta t^2}{\tau^2})\right] \tag{4}$$

Here, Δt is the difference between the observation and the estimation time and τ is the decorrelation time scale. The parameters L_0 and L_e are the zero-crossing and the e-folding length scales. The scalar r is the spatial separation distance.

The MSEAS OA is carried out in two stages. In the first stage, the largest dynamical scales are mapped onto computational grid using the parameters $(\tau,\, L_0,\, L_e)_{\mathrm{LS}}$. The background field for this stage is often chosen to be constant and equal to the horizontal mean of all the observations. In the second stage, the smaller scales are mapped using the coefficients $(\tau,\, L_0,\, L_e)_{\mathrm{ME}}$ often corresponding to the most energetic (meso) scales. The background field for this stage is the first stage OA. A major assumption in this OA approach is that the errors in the largest and the most energetic stages are statistically independent. The accuracy of the field estimates obtained using OA also depends on the spatial and time scale parameters used in the analytical correlation function, as well as the correlation function itself. The MSEAS OA approach has many similarities with the approach used for 'Levitus Climatology' (Levitus, 1982; Locarnini et al., 2006; Antonov et al., 2006; Garcia et al., 2006a,b), which is described in Appendix A.

The above approach for the MSEAS OA and 'Levitus Climatology', which are based on computing the covariance or the weight factors by providing the Euclidean distance as an input to the correlation function, are valid only for open oceans. So, the use of the optimal distance (the minimum distance between two points without going across complex landforms) is proposed to satisfy the coastline constraints. LSM or FMM, which are discussed in Section 4, can be utilized to obtain such optimal distance between any two points in a complex (e.g. multi-island) multiply-connected coastal region.

4. Methodologies for estimating the optimal path length in complex coastal regions and archipelagos

This Section describes the new methodologies for Objective Analysis, which are based on estimating the optimal path length (shortest path between

two points without going across landforms), in complex multiply-connected coastal regions. The new methodologies are based on finding the length of the optimal path using the Level Set Method and the Fast Marching Method. These methods are more accurate and computationally inexpensive as compared to the conventional Bresenham-based line algorithm (Bresenham, 1965) and Dijkstra's algorithm (Bertsimas and Tsitsiklis, 1997).

4.1. Objective Analysis using the Level Set Method (LSM)

A level set of a real-valued function ϕ of n variables is a set of the form:

$$\{(x_1, ..., x_n)|\phi(x_1, ..., x_n) = c\} \tag{5}$$

where, c is a constant. That is, a level set is the set where the function ϕ takes on a given constant value c.

Osher and Sethian (1988) proposed a numerical technique, which is called the Level Set Method, to implicitly represent and model the propagation of evolving interfaces under the influence of a given velocity field using appropriate partial differential equations (PDE's). An initial value formulation describing the interface motion is now discussed. The initial position of interfaces are given by level sets of the function ϕ. The evolution of this function ϕ is linked to the propagation of the interface through a time-dependent level set equation. Interfaces can be represented explicitly (parametrized interfaces i.e. interfaces given by $\mathbf{x} = \mathbf{x}(\mathrm{s})$, where s is the parameter) or implicitly (interfaces given by zero level set i.e. $\phi(\mathbf{x}) = 0$). Using the implicit representation $\phi(\mathbf{x})$, where $\mathbf{x}$ is the position vector, the convection equation can be solved to propagate level sets by a velocity field $\mathbf{v}$:

$$\phi_t + \mathbf{v}.\nabla\phi = 0 \tag{6}$$

In many cases, one is interested only in the motion normal to the boundary. Therefore, the velocity $\mathbf{v}$ can be represented using the scalar speed function F and the normal direction $\mathbf{n}$. Thus.

$$\mathbf{v} = F\mathbf{n} = F\frac{\nabla\phi}{|\nabla\phi|} \tag{7}$$

The hyperbolic, non-linear (Hamilton-Jacobi equation) level set equation, obtained from Equations 6 and 7, is given by:

$$\phi_t + F|\nabla\phi| = 0 \tag{8}$$

The following first order upwinded finite difference approximation can be used to numerically solve the level set equation (2-dimensional in space) (Osher and Sethian, 1988; Sethian, 1999b):

$$\phi_{i,j}^{n+1} = \phi_{i,j}^{n} - \Delta t[max(F,0)\nabla_{i,j}^{+} + min(F,0)\nabla_{i,j}^{-}]$$

where,

$$\begin{aligned}\nabla_{i,j}^{+} &= [max(D^{-x}\phi_{i,j}^{n},0)^2 + min(D^{+x}\phi_{i,j}^{n},0)^2 + \\ &\quad max(D^{-y}\phi_{i,j}^{n},0)^2 + min(D^{+y}\phi_{i,j}^{n},0)^2]^{1/2} \\ \nabla_{i,j}^{-} &= [min(D^{-x}\phi_{i,j}^{n},0)^2 + max(D^{+x}\phi_{i,j}^{n},0)^2 + \\ &\quad min(D^{-y}\phi_{i,j}^{n},0)^2 + max(D^{+y}\phi_{i,j}^{n},0)^2]^{1/2}\end{aligned} \tag{9}$$

Here, D^{-x} is the first order backward difference operator in the x-direction; D^{+x} is the first order forward difference operator in the x-direction, etc. Mathematically, these operators are given by:

$$D^{-x}\phi_{i,j} = \frac{\phi_{i,j} - \phi_{i-1,j}}{\Delta x}; \qquad D^{+x}\phi_{i,j} = \frac{\phi_{i+1,j} - \phi_{i,j}}{\Delta x} \tag{10}$$

The level set equation is an initial value problem which tracks the evolution of the level sets ϕ=constant assuming F is given by the specifics of the evolution of the ϕ for a particular problem.

If the scalar speed function of the front F is non-negative, then the steady state boundary value problem, known as the Eikonal equation, can be formulated to evaluate the arrival time function T($\mathbf{x}$). The Eikonal equation representing the time T($\mathbf{x}$) for the "frontal interface" to reach the position $\mathbf{x}$ from its initial position is given by:

$$F|\nabla T| = 1 \tag{11}$$

The Eikonal equation simply states that the gradient of the arrival time function is inversely proportional to the speed of the front. To solve the Eikonal equation, a time dependent problem is proposed. The time evolved steady state solution of the resultant Hamilton-Jacobi equation is the Eikonal equation. Mathematically, this is written as:

$$T_t + F|\nabla T| = 1 \xrightarrow{steady} F|\nabla T| = 1 \tag{12}$$

This Hamilton-Jacobi equation (Equation 12 (Left)) can be discretized using the numerical scheme for the Level Set equation. The steady state solution

of this Hamilton-Jacobi equation will be the solution of the Eikonal equation (Equation 12 (Right)).

The Level Set Method has been used in a wide variety of applications which include the arrival time problems in the control theory, generation of minimal surfaces, flame propagation, fluid interfaces, shape reconstruction etc. In the oceanic context, the method can be used to determine the optimal path length.

Numerics and operation count for the LSM: MATLAB code has been developed for Objective Analysis using the Level Set Method. For estimating the optimal distance, the scalar speed function F is set to 0 for the grid points on land and 1 for the grid points on water. The level set $T(\mathbf{x})$, which is the arrival time function, also represents the optimal distance from the starting position to the position vector $\mathbf{x}$ for the above speed function F. The above OA approach, which is based on computing the evolution of all the level sets and not simply the zero level set corresponding to the front itself, has an operation count of $O(N^3)$ in two dimensions for N^2 grid points (Sethian, 1999b). Thus, it is a computationally expensive technique since an extra dimension has been added to the problem.

A modified approach named 'Fast Marching level set method', which significantly reduces the operation count, is described next. Roughly speaking, the two possible ways to view these solution techniques are either iteration towards the solution, or direct construction of the stationary solution T. While LSM constructs the solution to the Eikonal equation (Equation 11) by iterating towards the solution, FMM is based on direct construction of the stationary solution T.

4.2. Objective Analysis using the Fast Marching Method (FMM)

The Fast Marching Method (FMM) for monotonically advancing fronts, which has been proposed by Sethian (1996, 1999b), is described. This method leads to an extremely fast scheme for solving the Eikonal equation (Equation 11). The Level set method relies on computing the evolution of all the level sets by solving an initial value partial differential equation using numerical techniques from hyperbolic conservation laws. As an alternative, an efficient modification is to perform the work only in the neighborhood of the zero level set, as this is known as the 'narrow band approach'. The basic idea of this alternative approach is to tag the grid points as either "alive", "land mines" or "far away" depending on whether they are inside the band, near its boundary, or outside the band, respectively. The work is performed only

on *alive* points, and the band is reconstructed once the land mine points are reached.

FMM, which allows boundary value problems to be solved without iterations, is now discussed in detail. The method is applicable to monotonically advancing fronts (i.e. the front speed ($F \geq 0$ or $F \leq 0$) which are governed by the level set equation (Equation 12). The steady state form of the level set equation is the Eikonal equation (Equation 11) which says that the gradient of the arrival time surface is inversely proportional to the speed of the front. For the two dimensional case, the stationary boundary value problem is given by:

$$|\nabla T| F(x,y) = 1 \quad s.t. \quad \Gamma = \{(x,y)|T(x,y) = 0\} \tag{13}$$

where Γ is the starting position of the interface. The first order finite difference discretization form of the Eikonal equation (Sethian, 1999b) at the grid point (i,j) is given by:

$$[max(D_{ij}^{-x}T,0)^2 + min(D_{ij}^{+x}T,0)^2 + \\ max(D_{ij}^{-y}T,0)^2 + min(D_{ij}^{+y}T,0)^2]^{1/2} = \frac{1}{F_{ij}}$$

or,

$$[max(max(D_{ij}^{-x}T,0), -min(D_{ij}^{+x}T,0))^2 + \\ max(max(D_{ij}^{-y}T,0), -min(D_{ij}^{+y}T,0))^2] = \frac{1}{F_{ij}^2} \tag{14}$$

Equation 14 is essentially a quadratic equation for the value at each grid point (assuming that values at the neighboring nodes are known). An iterative algorithm for computing the solution to Equation 14 was introduced by Ruoy and Tourin (1992). FMM is based on the observation that the upwind difference structure of Equation 14 means that the information propagates "one way", i.e. from the smaller values of T to the larger values. Therefore, FMM rests on solving Equation 14 by building the solution outward from the smallest time value T. The front is swept ahead in an upwind manner by considering a set of points in a *narrow band* around the existing front and bringing new points into the *narrow band* structure. The fast marching algorithm is discussed in detail in Appendix B.

The use of higher order FMM to reduce the error in the estimation of optimal path length is discussed in Section 7.2. Higher order FMM can

be useful in solving the divergence problems associated with our new OA scheme, but it is computationally expensive. These issues are discussed later in Sections 7.2 and 7.3.

Numerics and operation count for the FMM: MATLAB code has been developed for Objective Analysis using the Fast Marching Method. Once again, for estimating the optimal distance, the scalar speed function F is set to 0 for the grid points on land and 1 for the grid points on water. FMM has a significantly lower operation count of $O(N^2 \text{ Log } N)$ for N^2 grid points (Sethian, 1999b). Thus, it is a computationally inexpensive technique as compared to the Level Set Method.

The Fast Marching Method, as discussed above, is an efficient way to obtain the correlation between two locations by selecting the optimal path. The length of the optimal path computed using FMM or LSM can then be used for setting up the covariance matrix using the analytical correlation function (Equation 4).

4.3. Absolute velocity under geostrophic balance: Estimating the minimum vertical area in complex coastal regions and archipelagos

The optimization methodology for estimating the inter-island transport, proposed by Haley et al. (2009) is discussed in Appendix C. The objective of this methodology is to find a set of constant values for the transport streamfunction (Ψ) along the island coastlines that produce a suitably smooth initialization velocity field, e.g. with the fewest large velocity hot-spots, i.e. minimize the maximum absolute velocity in the initialized geostrophic flow field. Fortran-90 code from MSEAS (Haley, personal communication) has been modified to utilize the weight function based on the minimum vertical area between islands, which can be computed using the FMM/LSM. For obtaining the minimum vertical area, the scalar speed function in the Eikonal Equation (Equation 11) is chosen to be $F(x,y) = 1/H(x,y)$.

5. Objective Analysis using stochastically forced partial differential equations (SPDE's)

The use of Euclidean distance in the field covariance computed from the isotropic correlation function is not applicable in coastal regions since the complex the coastline constraints, e.g. there should be no direct relationship across landforms (islands, peninsulas etc.), need to be accounted. The

approach discussed in this section represents the field and its coastline constraints by a partial differential equation subject to stochastic forcing. The central idea of this approach, which is based on using stochastically forced partial differential equations (SPDE), is the numerical construction of a field covariance such that it accounts for the coastal constraints. The underlying field variability is represented as an outcome of a stochastic process using a SPDE and the stochasticity represents the uncertainty in this differential equation. For example, the stochastically forced Helmholtz equations in 1-D and 2-D in space for the field ψ in an unbounded domain (Balgovind et al., 1983) are associated with the following covariance functions respectively:

$$\begin{aligned} \frac{\partial^2\psi}{\partial x^2} - k^2\psi = \epsilon(x) \quad &\Leftrightarrow \quad C_{\psi\psi}(r) = (1+kr)e^{(-kr)} \\ \nabla^2\psi - k^2\psi = \epsilon(x,y) \quad &\Leftrightarrow \quad C_{\psi\psi}(r) = krK_1(kr) \simeq \left(\frac{\pi}{2}kr\right)^{1/2}\left(1+\frac{3}{8kr}\right)e^{-kr} \\ &\quad , \quad kr \to \infty \end{aligned} \tag{15}$$

where, K_1 is the Bessel function of the second kind. The process noise ϵ is a random disturbance with mean 0, standard deviation 1 and has no spatial correlation. Also, the length scale corresponds to the inverse of the SPDE parameter (k). Denman and Freeland (1985) have proposed other correlation functions which can also be linked to the appropriate SPDE's.

A major advantage of this SPDE approach is that the field-to-field covariance Cor($\mathbf{x}$,$\mathbf{x}$) can be computed numerically from the discretized SPDE along with appropriate boundary conditions (i.e. no flux boundary condition across islands) to directly account for the coastline constraints (Lynch and McGillicuddy, 2001). The discretization of SPDE (Equation 15) or any other differential operator on a finite element grid leads to the matrix form:

$$[A]\{\psi\} = \{e\} \tag{16}$$

All the coastline constraints are then incorporated automatically in this matrix form (16). Since $[C_{ee}] = [I]$, the covariance matrices for field-to-field points and field-to-data points are directly obtained from Equation 16:

$$\begin{aligned} Cor(\mathbf{x},\mathbf{x}) &= [A]^{-1}[C_{ee}][A]^{-T} = ([A]^T[A])^{-1} \\ Cor(\mathbf{x},\mathbf{X}) &= [A]^{-1}[C_{ee}][A]^{-T}[H]^T = ([A]^T[A])^{-1}[H]^T \end{aligned} \tag{17}$$

The covariance matrix (17) obtained using the SPDE approach can be used along with Gauss-Markov Estimation theory to perform Objective Analyses

in coastal regions. A limitation of this approach is that the resulting fields can be affected by the discretization error associated with the discretized form of the SPDE. In fact, we found that we often need to postprocess (smooth out) the SPDE-gridded fields to remove spurious field gradients. Such gradients, even when small, can lead to spurious velocities by aggregate integration in the vertical for the estimation of absolute velocity under geostrophic balance. It has also been verified that that the SPDE approach is computationally expensive when compared to our new FMM-based methodology.

A similar variant of the above methodology represents the covariance ($C_{\psi\psi}$), instead of the field (ψ), by a SPDE like Helmholtz equation (Logoutov, personal communication). Spatial variation in the resulting OA field are found to be more prominent with this new scheme (Agarwal, 2009). An heuristic reason is that this new representation corresponds to carrying out "smoothing" using the Helmholtz equation only once as compared to twice in the original representation. Both of these methods, the SPDE specified for the field (ψ) and the SPDE specified for the covariance ($C_{\psi\psi}$) were implemented in MATLAB (Logoutov personal communication).

Even though many different SPDE's could be utilized for mapping a field, in the example that follows, we selected the stochastically forced Helmholtz equation. First, the dynamics of the atmosphere can be approximately governed on the time scale of a few days by a Helmholtz-like equation, which is the equation for the conservation of potential vorticity under the assumptions of a quasi-geostrophic, frictionless, shallow water model without topography (Balgovind et al., 1983; Pedlosky, 1987). Second, the Helmholtz equation can be reduced from the diffusion or wave equations. In these linear PDE's, if the solution is assumed separable in time and space, one obtains for the time variation an ordinary differential equation of the first order. For the spatial variations, one always obtains the Helmholtz equation (Selvadurai, 2000), which is the equation that would be used for spatial mapping. Thirdly, the Helmholtz equation is equivalent to the steady diffusion-reaction equation.

In our examples in Equation 15, the SPDE parameter (k) is chosen such that the correlation function corresponding to the stochastically forced Helmholtz equation best fits the analytical correlation function used by the standard OA scheme and the LSM or FMM-based schemes (Section 4). These methods are compared to each other and to the LSM and FMM-based schemes in Section 6.2 using the World Ocean Atlas, 2005 data in the sub-domain of Philippines Archipelago.

6. Applications illustrating the novel OA methodologies

New methodologies for Objective Analysis in complex multiply-connected coastal regions were described in Section 4. These new methodologies are based on computing the optimal path lengths using the Level Set Method and the Fast Marching Method. These methods efficiently incorporate the coastline constraints (e.g. there is no direct relationship across landforms). The above methodologies are utilized to map the temperature, salinity and biological (chlorophyll) fields using a 2-staged mapping scheme in subsets of the following regions: Dabob Bay and Philippines Archipelago.

Section 6.1 evaluates the use of our new OA methodology in Dabob Bay and shows that it is more effective over other classic distance optimizing algorithms like Bresenham-based line algorithm (Bresenham, 1965). Section 6.2 shows a comparison of the different methodologies introduced in Section 4 and 5 for Objective Analysis in a subdomain of Philippines Archipelago. The estimation of absolute velocity under geostrophic balance by minimizing the inter-island transport is also illustrated.

6.1. Objective Analysis in Dabob Bay

Dabob Bay data are used to illustrate the effectiveness of the Fast Marching Method over other distance optimizing algorithms like Bresenham-based line algorithm (Bresenham, 1965). Maps for the temperature and salinity fields in a subdomain of Dabob Bay corresponding to the spatially irregular data in Figure 2 (Top) are obtained using the a. Bresenham-based line algorithm, b. Fast Marching Method. The limitation of Bresenham-based line algorithm is that the optimal distance computed using this method is discontinuous. This results in discontinuities in the covariance and also in the resultant field maps (Agarwal, 2009).

Figure 2 shows the temperature and salinity field maps in Dabob bay obtained using large length scales $(L_0 = 60,\ L_e = 30)_{\mathrm{LS}}$, most energetic length scales $(L_0 = 30,\ L_e = 15)_{\mathrm{ME}}$ and observational error $(R = 0.25I)$. Temperature and salinity have higher magnitudes in the northern part of the western arm of Dabob bay. The eastern arm of Dabob bay has relatively low temperature and salinity. Effects due to the discontinuity in distance obtained from Bresenham-based line algorithm is clearly evident in Figure 2 (Middle). Numerical fronts having high temperature and salinity gradients exist at the intersection of the two arms. Such fronts lead to numerical

problems in dynamical simulations. The geostrophic velocity obtained using these field maps will be unrealistic and will have high magnitudes along these fronts. A possible remedy, which reduces the discontinuity effects, is to smooth the distance by averaging distances of neighboring points (Haley, personal communication). The above averaging technique becomes numerically very expensive. The intensity of erroneous fronts are reduced in the field maps obtained using the averaged Bresenham-based line algorithm, but they still exist. Finally, the Fast Marching Method is used to compute distances and the Objective Analysis field maps obtained from our FMM-based scheme are clearly devoid of any numerical fronts (Figure 2 (bottom)). Along with that, FMM accurately satisfies the coastline constraints and it is computationally inexpensive compared to using the Bresenham-based line algorithm.

6.2. Objective Analysis in the Philippines Archipelago

This research study is motivated by the Philippines Straits Dynamics Experiment (PhilEx) sponsored by the Office of Naval Research. Novel OA techniques for such complex coastal regions are an important requirement to map very irregular datasets and initialize simulations. A comparison of the different OA methodologies will be illustrated in this region. We compare our new OA methods which are based on using a. Level Set Method and b. Fast Marching Method, to the a. Standard OA Method which ignores islands and uses the direct Euclidean distance and b. Stochastically forced partial differential equation approach (SPDE specified for the field).

A comparison of these methods using the World Ocean Atlas, 2005 (Locarnini et al., 2006; Antonov et al., 2006) data for the temperature and salinity field maps is discussed in this Section. WOA-05 data are data mapped using 'Levitus climatology' scheme (see Appendix A) and is regularly spaced. Regularly spaced WOA-05 data is used here primarily to illustrate and discuss the comparison of the different methodologies. Subsequently, synoptic in situ data is used. These real direct ocean data are the spatially irregular temperature, salinity and biology (chlorophyll) data.

6.2.1. Objective Analysis using WOA-05 data: Comparison of the different OA methodologies

Two-dimensional horizontal OA field maps, which correspond to the WOA-05 data in Figures 3-8 (Top-Left), are computed using methodologies proposed in Section 4 and 5. Figures 3, 4 and 5 show the temperature field maps at the depth of 0m, 200m and 1000m, respectively. Figures 6, 7 and

8 show the salinity field maps at the depth of 0m, 200m and 1000m, respectively. Large length scales $(L_0 = 540,\ L_e = 180)_{\mathrm{LS}}$ and most energetic length scales $(L_0 = 180,\ L_e = 60)_{\mathrm{ME}}$ are used with an observational error covariance $R = 0.25I$. For the SPDE approach, SPDE parameter $k = 1/200$ and observational error $(R = 0.25I)$ are used.

The OA field maps from all the methods (Figure 3 and 4) indicate that the Philippines Sea and the region near Palawan island is warmer than the rest of the region near the surface (0m, 200m). The region south of the Sulu sea around the Sulu Archipelago has relatively lower temperature. At levels below 500m (see Figure 5), there is a significant difference in the temperature of the Sulu sea (warm) as compared to the rest of the region (cold) (Gamo et al., 2007; Gordon, 2009). These temperature fields clearly show that direct correlation across landforms are weak. Similar observations can be made for Salinity. Salinity in the Sulu Sea and South China Sea (Figure 6 and 7) is lower than the salinity in the rest of the region near the surface (0m, 200m). At levels below 500m, the salinity in the Sulu sea (Figure 8) is significantly lower as compared to the rest of the region. These salinity fields further support the hypothesis that direct correlation across landforms are weak.

The field maps obtained using LSM and FMM are identical, but the FMM has a significantly lower computational cost. While LSM constructs the solution by iterating towards the solution, FMM is based on the direct construction of the stationary solution as described in Section 4. There is a very small difference in the field obtained using LSM and FMM because FMM exactly constructs the solution of the discretized Eikonal equation whereas LSM computes the solution within a desired tolerance limit. Thus, our OA methodology based on FMM should clearly be preferred, as it is more accurate and less expensive compared to OA methodology based on LSM.

The comparison of the temperature field maps and the salinity field maps obtained using different methods at level 1000m is shown in Figures 5 and 8, respectively. The methods based on FMM (Figures 3-8 (Bottom-Left)) and SPDE (Figures 3-8 (Bottom-Right)) clearly satisfy the coastline constraints. The data in the Sulu Sea, which has high temperature and low salinity compared to the remaining region, does not have any influence on the field outside the Sulu Sea since the two regions are not connected by water. On the other hand, the standard OA (Figures 3-8 (Top-Right)) does not satisfy the coastline constraints. Thus the data outside the Sulu Sea, where the temperature is low and salinity is high, is correlated to the field inside the Sulu Sea. This is undesirable since the direct relationship across

landforms is at best very weak. This leads to spurious high temperature and salinity gradients in the Sulu Sea, which will lead to problems for the estimation of geostrophic flow. Differences between temperature field maps and salinity field maps obtained using the FMM and using other OA methods at level 1000m are shown in Figure 9. There are small differences between field maps obtained using the FMM and SPDE approach because the analytical correlation function corresponding to the Helmholtz equation, which is used in the SPDE approach, is different from the analytical correlation function in the FMM. The differences between the field maps obtained using the FMM and standard OA are significantly large because the standard OA does not incorporate the coastline constraints.

The SPDE approach satisfies the coastline constraints, but the discretization errors in SPDE are significant and this results in prominent spatial variations in the temperature and salinity fields. The impact of such huge spatial variations on the geostrophic flow velocity is not good, and often additional smoothing has to be employed (post-processing) after obtaining the OA fields using the SPDE approach. Such post-processing is not required for our FMM-based scheme. The SPDE approach can be implemented by specifying the SPDE for the field or by specifying it for the covariance (Logoutov, personal communication). If the SPDE is specified for the field as opposed to the covariance, spatial variation in the field will be less prominent. Specifying the SPDE for the field will be more expensive than specifying the SPDE for the covariance, but this will make the spatial variation in the field less prominent and it will reduce the need for post-processing. Finally, we confirmed that the computational time required by the SPDE approach is higher than that of FMM. Thus, FMM appears to be the best among all the methodologies discussed in Section 4 and 5 for Objective Analysis in coastal regions. For mapping the spatially irregular data in the examples that follow, we will discuss the results of our FMM-based Objective Analysis scheme.

We now illustrate the estimation of absolute velocity under geostrophic balance in the Philippines Archipelago using the OA field maps. The algorithm for minimizing the inter-island transport (Appendix C) is utilized for computing a smooth geostrophic velocity flow field. We have utilized weight functions based on the minimum vertical area along each pair of islands in the algorithm for minimizing the inter-island transport. The estimation of the minimum vertical area has been carried out using the FMM by specifying the scalar speed function in the Eikonal equation (Equation 11) as F(x,y) = 1/H(x,y), where H is the ocean depth. The temperature and salinity data are

from the World Ocean Atlas 2005. They are mapped using our FMM-based OA scheme (Figures 3-8 (Bottom-Left)) and the SPDE approach (Figures 3-8 (Bottom-Right)), with the Helmholtz equation employed for the field. The streamfunction and velocity fields (at depths 0m, 100m) are shown in Figure 10. These streamfunction velocity plots obtained from the temperature and salinity field maps based on our FMM-scheme (Figure 10 (Left)) show a very good comparison with the streamfunction and velocity obtained using the temperature and salinity field maps based on the stochastically forced Helmholtz equation (Figure 10 (Right)). These maps suggest that the velocity is maximum in the Mindoro strait, near the Mindanao island and in the Balabac strait. The maximum absolute velocity, which is in the Balabac strait, is 79.7 cm/s. At lower depths, the velocity remain high in the Mindoro strait and near the Mindanao island. There is a large inter-island transport across the Mindoro strait since the vertical area between the Mindoro and Palawan island is very large.

Weight functions based on the minimum inter-island distance, which can be obtained using the FMM by specifying the scalar speed function in the Eikonal equation (Equation 11) as 1 for sea points and 0 for land points, were also used (Haley, personal communication). The velocity fields obtained using the weight functions based on the minimum inter-island distance has significantly large magnitudes, particularly in the Balabac strait (Agarwal, 2009). The maximum absolute velocity is 140.9 cm/s, which is significantly larger than the maximum absolute velocity obtained using weight functions based on the minimum vertical area (79.7 cm/s). Such high velocity magnitudes, which are obtained due to the inaccurate computation of inter-island transport, are clearly not acceptable. These results show that the weight functions based on the minimum vertical area will produce smooth geostrophic flow field with the least velocity hot spots.

6.2.2. Objective Analysis for Summer 2007: Melville exploratory cruise, sg122 and sg126 glider data

The data used in this example is collected from the Melville exploratory cruise, sg122 and sg126 gliders for the June-July'07 period. The data location plot is shown in Figure 11 (Top). Since the data is available only in a small region of the Philippines Archipelago near islands, Objective Analysis maps are computed in a portion of the regular Philex domain. Large length scales $(L_0 = 1080,\ L_e = 360)_{\mathrm{LS}}$, most energetic length scales $(L_0 = 270,\ L_e = 90)_{\mathrm{ME}}$ and observational error $(R = 0.2I)$ are used. The temperature

and salinity field maps obtained using the methodology based on the Fast Marching Method are shown in Figures 12 (Top) and 13 (Top), respectively at depths of 0m, 200m. Once again, these maps clearly indicate that the coastline constraints are appropriately satisfied. At depth of 0m, the warm region in the west of Luzon island is uncorrelated with the region on the east of Luzon island. The warm Sibuyan and Visayan Seas can be distinguished from the relatively cold Bohol Sea. At depths of 450m and 1000m, the data in the warm Sulu sea and Bohol Sea does not have any impact on the remaining regions, clearly suggesting that there is no direct relationship across landforms. Similar observations are made for the salinity. At depth of 0m, the low salinity region in the west of Luzon island is uncorrelated with the region on the east of Luzon island.

6.2.3. Objective Analysis for Winter 2008: Melville joint cruise data

The data used in this example is obtained from the joint Melville cruise for the Nov'07-Jan'08 period. The data location plot is shown in Figure 11 (Bottom). Large length scales $(L_0 = 1080,\ L_e = 360)_{\mathrm{LS}}$, most energetic length scales $(L_0 = 270,\ L_e = 90)_{\mathrm{ME}}$ and observational error $(R = 0.2I)$ are used for the OA field maps. The temperature and salinity field maps obtained using the FMM-based scheme are shown in Figures 12 (Bottom) and 13 (Bottom), respectively. Depths shown are 0m, 200m. Once again, at depth of 0m, the warm region in the west of Luzon island is uncorrelated with the region on the east of Luzon island. At depths of 450m and 1000m, the data in the warm Bohol Sea does not have any impact on the remaining regions, clearly suggesting that there is no direct relationship across landforms. Similar observations are made for salinity. At depth of 0m, the low salinity region in the west of Luzon island is uncorrelated with the region in the east of Luzon island.

We now compare fields in Winter 2008 from Melville joint cruise data with fields in Summer 20007 from Melville exploratory cruise, sg122 and sg126 glider data. It is clearly evident that the difference in temperature during Winter 2008 and Summer 2007 is more near the ocean surface. Beyond the depth of 200m, the difference is significantly less and the same inference is valid for salinity as well. At surface (0m), the temperature in the Sulu sea is nearly the same for both Summer 2007 and Winter 2008. But the temperature near Luzon island is significantly lower during Winter 2007 than the temperature during Summer 2007.

6.2.4. Objective Analysis for biological field (chlorophyll)

Application of our new FMM-based scheme for the biological field (chlorophyll) is illustrated here using Exploratory cruise Summer 2007 data. The biological OA field map obtained can be utilized in the initialization for coupled physics-biology modeling studies (Burton, 2009). Large length scales $(L_0 = 1080, L_e = 360)_{\mathrm{LS}}$, most energetic length scales $(L_0 = 270, L_e = 90)_{\mathrm{ME}}$ and observational error $(R = 0.2I)$ are used for the OA field maps. The chlorophyll maps computed using our FMM-based scheme are shown in Figure 14 at depths of 0m, 10m, 50m, 160m. The concentration of biological fields like chlorophyll, phytoplankton and zooplankton is substantial only near the surface due to the presence of sunlight. Therefore, the coupled physics-biology modeling studies are usually carried up to the depth of 200m.

The chlorophyll concentration is maximum near islands. Away from islands, it approaches the mean data value. At depth of 0m and 10m, the maximum chlorophyll concentration is observed in the south of the Visayan sea and in the Bohol Sea. At a depth of 50m, the chlorophyll concentration in the south of the Visayan sea and in the Bohol Sea remains significant. The maximum chlorophyll concentration is observed in the north of Palawan island. The biological concentration at lower depths decreases very rapidly.

This concludes the demonstration of the new OA methodologies and the methodology for obtaining the geostrophic flow velocities in complex coastal regions. The computational details of the OA methodologies will be discussed in Section 7.

7. Computational Analysis

Computational studies of properties of new mapping schemes are carried out in this Section. The sequential processing of observations (see Parrish and Cohn (1985); Cho et al. (1996)) is employed for mapping irregular data using our new OA schemes. Sequential processing reduces computational costs and it also allows to estimate the impact of individual data. The comparison of computational costs for the OA schemes is made in Section 7.1.

It is known that the Kalman Filter encounters divergence problems if the covariance matrix is negative (Brown and Hwang, 1997). Analytical correlation functions, which are used to generate covariance matrix, are termed "positive definite correlation functions" if they generate positive definite covariance matrix using the Euclidean distance for a simply-connected convex domain. It has been well established using the Wiener-Khinchin and

Bochner's theorems that if a Fourier transform (or the spectral density of a correlation function) is non-negative for all frequencies then the correlation function is positive definite (Yaglom, 1987; Papoulis, 1991; Yaglom, 2004; Dolloff et al., 2006). For complex coastal regions, Cor($\mathbf{x}$,$\mathbf{x}$) generated from "positive definite correlation functions" may not necessarily be positive definite due to: a. numerical error in the computation of the optimal path length using FMM/LSM b. the presence of landforms (Agarwal, 2009). This may lead to divergence problems for the field mapping based on the FMM/LSM scheme in complex coastal regions. Such divergence problems are illustrated using the WOA-05 data (Spliced February and Winter Climatology) shown in Figure 15 (Top-Left). The field maps obtained using our FMM-based scheme (one-scale) with length scales ($L_0 = 540$, $L_e = 180$) and length scales ($L_0 = 1080$, $L_e = 360$) are shown in Figure 15. Fields obtained using the larger scales (Figure 15 (Bottom-Left)) clearly show divergence problems near the Palawan island. Such problems are not encountered when the smaller length scales are used (Figure 15 (Top-Right)). Specifically, questions which motivate our research in Section 7.2 and 7.3 are: a. What are the computational errors in optimal path lengths computed using the FMM/LSM and how can they be reduced? b. What are the computational issues including non-positive definite covariances that arise in a multiply-connected coastal domain and how can they be remedied? A higher-order Fast Marching Method than the first-order one (Section 4.2) is discussed in Section 7.2. Higher-order FMM results in a significant reduction of errors in the distance estimates, i.e. the difference between the numerically computed and the true optimal distances and helps in dealing with the divergence problems to some extent. In Section 7.3, methods to deal with negative covariances arising due to the presence of islands and due to the numerical error in computing the optimal path length are discussed.

7.1. Comparison of Computational Costs

For a 2-dimensional domain with N points in each direction, a comparison of the operation count for computing the optimal distance from a data location to all other grid points in the domain using different Methods is given in Table 2.

There are a total of N^2 grid points at each level and the operation count for LSM is obtained from an optimistic guess that LSM will take roughly N steps to converge. In reality, the iterations can take much longer to converge, and therefore LSM is not a very efficient method for computing the optimal

Method	Operation Count
Level Set Method	O(N^3)
Fast Marching Method	O($N^2 logN$)
Dijkstra's Method	O(N^3)

Table 2: Comparison of the operation count for the optimal distance obtained using LSM, FMM and Dijkstra's Method.

distance to perform OA. On the other hand, FMM is an efficient technique which requires a fast method to locate the smallest value grid point in the *narrow band*. The Min-Heap data structure with backpointers (Sedgewick, 1988) is employed to efficiently locate the grid point with the minimum value. The total work done in the DownHeap and UpHeap operations, which ensure that the updated quantities do not violate the heap properties, is O(log N). Thus 2-dimensional FMM with N grid points in each direction has an operation count of $N^2 logN$, which is a significant improvement over LSM. We also observe that the FMM-based OA requires less computational time (approximately 15 %) than the OA based on SPDE approach. Thus, the FMM-based OA is computationally the most efficient technique for mapping in complex multiply-connected domains.

7.2. Higher order Fast Marching Method

In a domain with no islands or landforms, the optimal path length obtained using the FMM/LSM should ideally be equal to the Euclidean distance. But the numerical estimation of the optimal path length using the FMM/LSM has discretization errors and this leads to an inaccurate estimation of the optimal path length. The Weiner Khinchin and Bochner theorems are valid for covariances computed using the Euclidean distance in a simply-connected convex domain. The covariance matrix may no longer be positive definite due to the inaccurate computation of the optimal path length by FMM/LSM or due to the presence of islands. This may lead to divergence problems in the resultant field maps. Specifically, the question which motivates this Section is: What are the computational errors in the optimal path lengths computed using the FMM/LSM and how can they be reduced? Here, we introduce the higher order Fast Marching Method which will reduce errors in the estimation of the optimal path length.

The Fast Marching Method presented in Section 4.2 is a first order scheme, since the first order discretization form (Equation 14) of the Eikonal equation (Equation 11) was used. A different implementation of FMM with higher accuracy (Sethian, 1999a,b) is discussed here. Note that the second order backward approximation to the first derivative T_x is given by:

$$T_x \approx \frac{3T_i - 4T_{i-1} + T_{i-2}}{2\Delta x} \Leftrightarrow T_x \approx D^{-x}T + \frac{\Delta x}{2} D^{-x-x}T \tag{18}$$

Similarly, the second order forward approximation to the first derivative T_x is given by:

$$T_x \approx \frac{3T_i - 4T_{i+1} + T_{i+2}}{2\Delta x} \Leftrightarrow T_x \approx D^{+x}T - \frac{\Delta x}{2} D^{+x+x}T \tag{19}$$

Here D^{-x} and D^{+x} are the first order forward and backward approximations for the first derivative, respectively (Equation 10), $D^{-x-x} \equiv D^{-x}D^{-x}$and $D^{+x+x} \equiv D^{+x}D^{+x}$.

Consider the switch functions defined by:

$$\begin{aligned} switch_{ij}^{-x} &= \begin{pmatrix} 1 & \text{if } T_{i-2,j} \text{ and } T_{i-1,j} \text{ are known ('Alive')} \\ & \qquad \text{and } T_{i-2,j} \leq T_{i-1,j} \\ 0 & \qquad \text{otherwise} \end{pmatrix} \\ switch_{ij}^{+x} &= \begin{pmatrix} 1 & \text{if } T_{i+2,j} \text{ and } T_{i+1,j} \text{ are known ('Alive')} \\ & \qquad \text{and } T_{i+2,j} \leq T_{i+1,j} \\ 0 & \qquad \text{otherwise} \end{pmatrix} \end{aligned} \tag{20}$$

Similar functions are defined in the y-direction. The higher accuracy scheme attempts to use a second order approximation for the derivative whenever the points are tagged as 'alive' (the points inside the band where the value of the arrival time function is frozen: see Section 4.2) but reverts to the first order scheme otherwise.

The modified discretization equation for the higher accuracy FMM is

given by:

$$\begin{pmatrix} max([D_{ij}^{-x}T + switch_{ij}^{-x}\frac{\Delta x}{2}D_{ij}^{-x-x}T], \\ -[D_{ij}^{+x}T - switch_{ij}^{+x}\frac{\Delta x}{2}D_{ij}^{+x+x}T], 0)^2 \\ + \\ max([D_{ij}^{-y}T + switch_{ij}^{-y}\frac{\Delta y}{2}D_{ij}^{-y-y}T], \\ -[D_{ij}^{+y}T - switch_{ij}^{+y}\frac{\Delta y}{2}D_{ij}^{+y+y}T], 0)^2 \end{pmatrix} = \frac{1}{F_{ij}^2} \tag{21}$$

It should be noted that the above scheme is not necessarily a second order scheme. The accuracy of the above scheme depends on how often the switches evaluate to zero and how the number of points where the first order method is applied changes as the mesh is refined. When the number of points where the first order method is applied is relatively small (occurs only near the coastlines), the error is reduced considerably by using the higher accuracy FMM. It should also be noted that a third or higher-order approximations for the derivative T_x can similarly be used to construct more accurate FMM schemes, but this will increase the computational cost. Also, the error percentage in the optimal distance computed using FMM is higher near the data point and it reduces as the distance increases. To keep the computational cost low and a uniform error percentage, one can use higher accuracy FMM near the data point and then progressively shift to the lower order schemes as the distance increases.

The higher order Fast Marching Method has been used to minimize errors in the estimation of the optimal path length in Philippines Archipelago. Figure 15 (Bottom-Right) clearly shows that the use of higher order Fast Marching Method has attenuated the divergence problems compared to the first order FMM. The divergence problems do not vanish completely because of the presence of landforms and due to discretization errors associated with higher order FMM. We introduce other methods to deal with such divergence problems for multiply-connected coastal domains in Section 7.3.

7.3. Positive Definite covariance matrix for complex multiply-connected coastal regions

Apart from the inaccurate optimal path length, the covariance matrix may also become negative due to the presence of islands and coastlines. Specifically, the question which motivates this Section is: What are the computational issues including non-positive definite covariances that arise in a

multiply-connected coastal domain and how can they be remedied? The presence of islands and archipelagos results in stretching of the Euclidean path, which can potentially make the covariance matrix negative. Examples of this will be shown next. Possible remedies to deal with the negative covariance matrix, which lead to divergence problems, are then discussed (Agarwal, 2009).

Consider the idealized multiply-connected domain having an island, shown in Figure 16. This domain has 12 grid points which are marked as ocean points and 4 grid points which are marked as land points. The length of the optimal path is computed exactly to form the covariance matrix to keep it untouched from effects due to discretization errors in the FMM/LSM. The positive-definite correlation function $Cor(r) = exp\left[-\frac{r^2}{2L^2}\right]$ with L=2 is used to form the covariance matrix. We find that the covariance matrix is not positive definite. The maximum eigen value for the covariance matrix is 6.3345 while the minimum is -0.0504. This idealized example clearly shows that the covariance matrix based on the optimal path length for a complex multiply-connected region may not necessarily be positive definite.

Methods that can be used to remove the divergence problems (Figure 17 (Top-Left)) due to the negative covariance matrix are:

a. Discarding the problematic data: One method to deal with the problem of a negative covariance matrix is to discard the data corresponding to the negative values of $H_j Cor(\mathbf{x}, \mathbf{x})_{j-1} H_j^T$. Even though, this will ensure that there are no divergence issues in the resultant OA, this method is a not the most acceptable one since the information in the data is discarded entirely. The field map obtained by discarding the problematic data is shown in Figure 17 (Top-Right). Clearly, the divergence problems are removed but loosing all the information in the data is not acceptable.

b. Introducing process noise: Adding a small process noise to the diagonal elements of the covariance matrix helps in dealing with the divergence problems associated with a negative covariance matrix (Brown and Hwang, 1997). The disadvantage is that the process noise introduced will lead to a degree of sub-optimality. It is often a more acceptable method compared to discarding the data. Once again, the field map obtained by introducing the process noise is free from the divergence problems and the resulting field is shown in Figure 17 (Bottom-Left).

c. Dominant Singular Value Decomposition (SVD) of a-priori covariance: To construct the OA field maps, the full covariance matrix is not

required. The computation of the full covariance matrix (Cor($\mathbf{x}$,$\mathbf{x}$)) is expensive and it is therefore rarely done for the OA in complex coastal regions. The necessary requirement to obtain the field maps is the matrix corresponding to the grid and the data point covariance (Cor($\mathbf{x}$,$\mathbf{X}$)). The divergence problems in the Kalman update or in the sequential processing of observations can be removed by first obtaining the singular value decomposition (SVD) of Cor($\mathbf{x}$,$\mathbf{X}$) and then reconstructing the new covariance matrix by retaining only the dominant singular values and setting the smaller singular values (less than 1 percent of the maximum singular value) to zero. The above procedure will make the covariance positive definite. It has been verified that the magnitude of the negative eigen values in the covariance matrix is very small compared to the magnitude of the maximum eigen value. This verification establishes that the use of the dominant singular value decomposition method is the most acceptable method to remove the divergence problems in the update because it looses the least information contained in the data. Once again, the field map obtained by dominant singular value decomposition (SVD) of a-priori covariance is free from divergence problems and the plot is shown in Figure 17 (Bottom-Right). It has also been verified that the fields obtained by introducing the process noise and the fields obtained by applying the dominant singular value decomposition of the a-priori covariance are similar.

8. Summary and Conclusions

Our research consisted of the following related investigations: a. new methodologies for the mapping and dynamical inference of ocean fields from irregular data in complex multiply-connected domains, and b. computational studies of properties of the new mapping schemes. Results, findings and future work are summarized next.

New methods for efficient field mapping, i.e. Objective Analysis, in complex coastal regions were researched, implemented and utilized. These new OA methods, which satisfy the coastline constraints (e.g. there is no direct relationship across landforms), are based on estimating the length of the optimal path using either the Level Set Method (LSM) or the Fast Marching Method (FMM). These novel methods were applied and studied in complex domains of the Philippines Archipelago and Dabob Bay using realistic datasets to obtain field estimates such as temperature, salinity and biology (chlorophyll). Results were compared with those of a standard OA scheme

(using across-landforms Euclidean distance in the analytical correlation function) and of OA schemes based on the use of stochastically forced partial differential equations (SPDE). We have shown that our new FMM-based scheme is computationally inexpensive compared to our LSM-based scheme and the SPDE approach. Our illustrations and studies show that the field maps obtained using our FMM-based scheme do not require postprocessing (smoothing) of fields e.g. they are devoid of any spurious hydrographic field gradients which are unacceptable for flow computation. The use of FMM is the most appropriate method for the optimal distance estimation among the distance estimation methodologies like Dijkstra's optimization algorithm and the classic Bresenham-based line algorithm. The optimal distance computed using Dijkstra's algorithm is computationally expensive and inaccurate. Apart from being computationally expensive, the optimal distance computed using the Bresenham line algorithm is discontinuous. This results in the formation of fronts with high field gradients. Such high gradient fronts do not occur when our FMM-based scheme is utilized.

Computational studies of properties of the new mapping schemes were carried out. The sequential processing of observations reduces the computational cost and also helps in understanding the impact of individual data. Wiener-Khinchin and Bochner theorem are valid only for the correlation functions based on the Euclidean distance for convex simply-connected domains. It was found that the covariance matrix is no longer positive definite when the optimal path length is computed using FMM. Therefore, the use of high order FMM was discussed and implemented to obtain more accurate length of shortest sea paths. However, we found that the covariance matrix also becomes negative due to the presence of islands and other non-convex landforms. Several approaches to overcome this issue were discussed. These include discarding problematic data points, introducing process noise, and reducing the covariance matrix by applying the dominant singular value decomposition (SVD). Among these, we argue that introducing process noise and reducing the covariance matrix by applying the dominant SVD are the best solutions.

We have also discussed our new FMM based methodology for the estimation of absolute velocity under geostrophic balance in complex multiply-connected domains. FMM is used for the computation of the minimum vertical area between all pairs of islands. The minimum area is required for obtaining the transport streamfunction which minimizes the inter-island transport and produces a smooth velocity flow field. The transport streamfunction

can then be utilized to estimate the geostrophic flow velocity from the temperature and salinity field maps alone. We have illustrated this method by applying it in a subdomain of the Philippines Archipelago.

One of the things we have started to investigate is to utilize our FMM-based OA scheme for incorporating the non-homogeneous dynamical effects, but much work remains to be done. We have appropriately modified the scalar speed function in the Eikonal equation. In particular, we may have a bathymetry-dependent scalar speed function to include bathymetric effects at lower depth levels. We also propose to use the smallest length scale on the optimal path to include the non-homogeneous effects due to the existence of fronts in a continental shelf. Analogous modification of the scalar speed function or the length scale can be used to incorporate other dynamical effects (e.g. conservation of potential vorticity). The optimal path length obtained using our FMM/LSM-based scheme can also be used to extend the methodology proposed by Lermusiaux et al. for three-dimensional, multivariate and multi-scale spatial mapping of geophysical fields and their dominant errors (Lermusiaux et al., 1998, 2000; Lermusiaux, 2002) to complex coastal regions. This method reduces the dimension of the error covariance matrices by focusing on the error subspace formed by dominant eigen-decomposition of the a-priori covariance (Lermusiaux and Robinson, 1999). Three-dimensional, multivariate and multi-scale spatial mapping using our FMM based scheme is also a subject of further research.

A. Objective Analysis approach for 'Levitus Climatology'

The objective analysis scheme used for 'Levitus Climatology' (Levitus, 1982; Locarnini et al., 2006; Antonov et al., 2006; Garcia et al., 2006a,b) has its origins in the work of Cressman (1959) and Barnes (1964). This scheme is based on adding "corrections", which are computed as a distance-weighted mean of all grid point difference values, to the first-guess field. Initially, the World Ocean Atlas 1994 (WOA94) used the Barnes (1973) scheme which requires only a single "correction" to the first-guess field at each grid point in comparison to the successive correction method of Cressman (1959) and Barnes (1964). This was done to reduce the computing time. Barnes (1994) suggests using the multi-pass analysis when computing time is not an issue. The analysis scheme used in WOA98, WOA01 and WOA05 is a three-pass "correction" scheme. The inputs to this analysis scheme are one-degree square means of the observed data values, and a first-guess field. The differ-

ence between the observed mean and the first-guess field is then computed. An influence radius is specified next and a correction to the first-guess value at all the grid points is computed as a distance-weighted mean of all the grid point difference values that lie within the area around the grid point defined by the influence radius. Mathematically, the correction factor derived by Barnes (1964) is given by:

$$C_{i,j} = \frac{\sum_{s=1}^{d} W_s Q_s}{\sum_{s=1}^{d} W_s} \tag{22}$$

where,
(i, j) - coordinates of a grid point in east-west and north-south directions respectively;
$C_{i,j}$ - correction factor at the grid point coordinates (i, j);
d - the number of data points that fall within the area around point (i, j) defined by the influence radius;
Q_s - difference between the observed mean and the first-guess at the Sth data point in the influence area;
$W_s = exp(-Er^2/R^2)$ (for $r \leq R$; $W_s = 0$ for $r > R$) $\equiv$ Correlation weight;
r - distance of observation from the grid point;
R - influence radius;
$E = 4$.
At each grid point, the analyzed value $G_{i,j}$ is the sum of the first guess $F_{i,j}$ and the correction $C_{i,j}$. The expression is:

$$G_{i,j} = F_{i,j} + C_{i,j} \tag{23}$$

If there is no data within the area defined by the influence radius, the correction is zero and the analyzed value of the field is the same as the first-guess. The analysis scheme is set up such that the inference radius can be varied in each iteration. To progressively analyze the smaller scale phenomena with each iteration, the analysis begins with a large inference radius which is decreased gradually with each iteration.

Equation 23 can also be expressed in the matrix form, which is given by

$$\mathbf{G} = \mathbf{F} + [diag(\mathbf{W}\mathbf{e}_d)]^{-1}\mathbf{W}\mathbf{Q} \tag{24}$$

Here n is the number of model points, the analyzed field $\mathbf{G}$ and the first guess $\mathbf{F}$ are n-by-1 vectors, the correlation weight matrix $\mathbf{W}$ is a n-by-d matrix,

the difference between the observed mean and the first-guess at the data point $\mathbf{Q}$ is a d-by-1 vector and $\mathbf{e}_d$ is a d-by-1 vector with unit entities. The operation diag($\mathbf{v}$) creates a diagonal matrix i.e. it puts the vector $\mathbf{v}$ on the main diagonal.

Analogous to the Kalman Gain ($\mathbf{K}$) from the Gauss Markov criterion ($K = Cor(\mathbf{x}, \mathbf{X})[Cor(\mathbf{X}, \mathbf{X}) + \mathbf{R}]^{-1}$), Equations 24 and 1 show that a similar Gain matrix ($K_L = [diag(\mathbf{W}\mathbf{e}_d)]^{-1}\mathbf{W}$) can be defined for the Levitus methodology. While the multi-scale OA approach in MSEAS is based on Gauss Markov estimation theory, the Levitus OA is based on estimating the field by computing the distance-weighted mean of all grid point difference values (between the mean and first-guess field) in the inference radius and then adding it to the first-guess field. Thus, the choice of the first guess-field is very important in the 'Levitus OA' analysis. On the other hand, in Gauss Markov estimation, the first-guess field is often the mean of the data values and the correction is made in the Kalman update step by computing the difference between the data and the interpolated value of the first-guess on the data location. The Gauss Markov estimation theory also requires the knowledge of the observation noise or error covariance of the data ($\mathbf{R}$).

B. Fast Marching Algorithm

The fast marching algorithm (Sethian, 1996, 1999b) is:

1. Initialize
   (a) *Alive* points: Let A be the set of all grid points (i,j) on the starting position of the interface Γ; set $\mathrm{T_{ij}} = 0$ for all points in A.
   (b) *Narrow Band* points: Let the *Narrow Band* be the set of all grid points (i,j) in the immediate neighborhood of A; set $T_{ij} = \frac{d}{F_{ij}}$ for all points in the *Narrow Band* where, d is the grid separation distance.
   (c) *Far Away* points: Let the *Far Away* region be the set of all remaining grid points (i,j); set $T_{ij} = \infty$ for all points in the *Far Away* region.
2. Marching Forward
   (a) Begin Loop: Let (i_{min},j_{min}) be the point in the *Narrow Band* with the smallest value for T.
   (b) Add the point (i_{min},j_{min}) to A; remove it from the *Narrow Band*.

(c) Tag as neighbors any points ($i_{min}-1$,j_{min}), ($i_{min}+1$,j_{min}), (i_{min},$j_{min}-1$), (i_{min},$j_{min}+1$) that are either in the *Narrow Band* or the *Far Away* region. If the neighbor is in the *Far Away* region, remove it from that list and add it to the *Narrow Band*.

(d) Recompute values of T at all neighbors in accordance with Equation 14. Select the largest possible solution to the quadratic equation.

(e) Return to the top of the loop.

Here are some properties of the fast marching algorithm. The smallest value in the *Narrow Band* is always correct. Other *Narrow Band* or *Far Away* points with larger values of T cannot affect the smallest value. Also, the process of recomputing T values at the neighboring points cannot give a value smaller than any of the accepted value at *Alive points*, since the correct solution is obtained by selecting the largest possible solution to the quadratic equation (Equation 14). Thus the algorithm marches forward by selecting the minimal T value in the *Narrow Band* and recomputing the values of T at all neighbors in accordance with Equation 14.

The key to an efficient version of the algorithm lies in finding a fast way to locate the grid point in the *Narrow Band* with the minimum value for T. To do so, the heapsort algorithm (Williams, 1964; Sedgewick, 1988) with backpointers is often implemented and it is the algorithm we used here. This sorting algorithm generates a "complete binary tree" with the property that the value at any given parent node is less than or equal to the value at its child node. Heap is represented sequentially by storing a parent node at the location k and its child at locations $2k$ and $2k+1$. The member having the smallest value is stored at the location $k=1$.

All *Narrow Band* points are initially sorted in a heapsort. The fast marching algorithm works by first finding, and then removing, the member corresponding to the smallest T value from the *Narrow Band* which is followed by one sweep of DownHeap to ensure that the remaining elements satisfy the heap property. The DownHeap operation moves the element downwards in the heap till the new heap satisfies the heap properties. *Far Away* neighbors are added to the heap using the Insert operation which increases the heap size by one and brings the new element to its correct heap location using the UpHeap operation. The UpHeap operation moves the element upwards in the heap till the new heap satisfies the heap properties. The updated values at the neighbor points obtained from Equation 14 are also brought to the

correct heap location by performing the UpHeap operation.

C. Estimation of the absolute velocity under geostrophic balance by minimizing the inter-island transport

For ocean flows, which evolve over long spatial-time scales and away from the immediate vicinity of the sea-surface, the dominant terms in the horizontal momentum equations are the terms corresponding to the Coriolis force and the pressure gradient. Such a flow field, where a balance is struck between the Coriolis and the pressure forces, is called geostrophic. The thermal wind equations are obtained for geostrophic flow by assuming that the vertical momentum equation is approximately given by hydrostatic balance. The thermal wind equations are:

$$-f\frac{\partial(\rho v)}{\partial z} = g\frac{\partial \rho}{\partial x} \quad and \quad f\frac{\partial(\rho u)}{\partial z} = g\frac{\partial \rho}{\partial y} \tag{25}$$

where, ρ is the density, u and v are the horizontal fluid velocity in the zonal (x) and meridional (y) directions respectively, and $f = 2\Omega\ sin\phi$ is the Coriolis parameter for the spherical earth rotating at a rate of Ω at latitude ϕ. The thermal wind equations (Equation 25) when integrated in the vertical give:

$$\begin{aligned} \rho v(x,y,z,t) &= \frac{-g}{f}\int_{z_0}^{z}\frac{\partial \rho}{\partial x}dz + \rho v_0 \\ \rho u(x,y,z,t) &= \frac{g}{f}\int_{z_0}^{z}\frac{\partial \rho}{\partial y}dz + \rho u_0 \end{aligned} \tag{26}$$

where, z_0 or the level of no motion for $v_0, u_0 = 0$ or a level of reference for $v_0, u_0 \neq 0$.

Flow estimation based on thermal wind balance (Equation 26), is a classical problem in physical oceanography (Wunsch, 1996). Historically, the only significant routine measurements possible were the temperature, T, and salinity, S, of the water at various depths. The equation of state for seawater then permits the estimation of density at a given pressure from the temperature and salinity measurements. Thus the geostrophic flow can be computed using the above method (Equation 26) from the shipboard measurements of T and S alone. The formulation has been well defined for the open oceans without any landforms. For complex coastal regions having landforms such as islands and peninsulas, estimation of the inter-island transport is first required before proceeding with the geostrophic formulation discussed above.

The optimization methodology for estimating the inter-island transport, proposed by Haley et al. (2009) is utilized and discussed below. The objective of this methodology is to find a set of constant values for the transport streamfunction (Ψ) along the island coastlines that produce a suitably smooth initialization velocity field, e.g. with the fewest large velocity hot-spots, i.e. minimize the maximum absolute velocity in the initialized geostrophic flow field. The working assumptions for Haley's methodology are listed below:

1. Coastlines in the given domain can be divided into two distinct subsets:

(a). Set A: N coastlines along which the transport streamfunction is unknown, $N \neq 0$.

(b). Set B: M coastlines along which the transport streamfunction is known.

2. The solution for the transport streamfunction Ψ_0 exists for the case which includes coasts in set B, but coasts in set A, along with the corresponding interiors, are replaced by open ocean (e.g. island sunk to 10m depth).

3. The difference between the initial solution Ψ_0 and the final solution Ψ is not extremely large. Otherwise, the information from Ψ_0 would not be accurate enough.

Ψ_0 contains useful information like the relative position of major currents to various coastlines and the effects of topography on the flow. Thus, the information in Ψ_0 can be utilized to estimate the constant value of the transport streamfunction along the island coastlines by constructing an optimization functional for minimizing the inter-island transport subject to weak constraints. Haley's methodology for constructing the optimization functional is now discussed.

The problem is divided into three parts to construct the optimization functional. The optimization functional (E) in the general form, which is a summation of three terms, is given by:

$$E = E_1 + E_2 + E_3 \tag{27}$$

where, E_1 is the minimizing target for the transport between all pairs of the unknown (Set A) coasts, E_2 is the minimizing target for the transport between all pairs of unknown (Set A) and known (Set B) coasts and E_3 is the minimizing target for the transport between all pairs of the unknown (Set A) coasts and the open boundaries of the domain. Detailed expressions for E1, E2 and E3, which also requires the use of appropriate weight functions (w_{nm}

for the pair of islands denoted here by subscripts n and m), are provided by Haley et al. (2009). The minimum of E is computed by solving the standard least square problem i.e by setting gradients with respect to the unknowns variables (transport streamfunction values along the island coastlines) equal to zero. These streamfunction values, which smooth the velocity field, will be used as Dirichlet boundary conditions while solving the geostrophic flow equations using the Temperature and Salinity OA maps. The illustration of this methodology in the complex domain of Philippines Archipelago is discussed in Section 6.2.

Suitable weight functions are required to construct the optimization function (E). Consider the stream function (Ψ) for a two-dimensional horizontal flow. It is defined such that the flow velocity can be expressed as:

$$\vec{u} = (u, v) = \frac{1}{H}\nabla \times \Psi\hat{k} \Rightarrow u = \frac{1}{H}\frac{\partial \Psi}{\partial y}, v = -\frac{1}{H}\frac{\partial \Psi}{\partial x} \tag{28}$$

Here, H is the ocean depth. The transport between a pair of islands having streamfunction ψ_1 and ψ_2 is given by:

$$\psi_2 - \psi_1 = \int_A \vec{u}.\hat{n}dA \tag{29}$$

where, A is the vertical area between the two islands and $\hat{n}$ is the unit vector normal to the vertical area. Equation 28 and 29 suggests that the appropriate weight function to smooth the velocity field should be $w_{nm} = 1/A_{nm}^2$, where, A_{nm} is the minimum vertical area along any path between the two islands (denoted here by subscripts n and m). Another heuristic choice of weight function can be $w_{nm} = 1/d_{nm}^2$, but this will be appropriate when the ocean depth is uniform in between all pairs of islands. Since the ocean depth is not uniform, a new methodology is required to compute the minimum area along any path between a pair of islands. Using the Fast Marching Method (FMM), which was described in Section 4.2, is a very convenient and efficient way to compute A_{nm}. Simulations have been performed with several other weight functions to confirm that the proposed weight function based on the minimum vertical area (A_{nm}) is the most appropriate for smooth velocity flow field with minimum hot-spots.

D. Acknowledgments

We are sincerely thankful to Dr. Patrick J. Haley and Wayne G. Leslie for providing us with data, computational codes and very helpful inputs. We

are very thankful to Oleg G. Logoutov for sharing his methods and ideas. We are very grateful to the whole Philex and PLUSNet teams for their fruitful collaborations. In particular, we thank crews, operators and support personnel of the Melville ship (Prof. Arnold L. Gordon, Lamont-Doherty Earth Observatory of Columbia University), gliders (University of Washington - Applied Physics Laboratory: Craig Lee, Bruce Howe, Marc Stewart) and kayaks (MIT LAMSS group under the guidance of Prof. Henrik Schmidt) for their work and the critical data they provided.

References

Agarwal, A., 2009. Statistical field estimation and scale estimation for complex coastal regions and archipelagos. SM Thesis, Massachusetts Institute of Technology.

Antonov, J. I., Levitus, S., Boyer, T. P., Conkright, M. E., OBrien, T. D., Stephens, C., 1998a. World ocean atlas 1998 volume 1: Temperature of the atlantic ocean. NOAA Atlas NESDIS 27. US Government Printing Office: Washington, DC.

Antonov, J. I., Levitus, S., Boyer, T. P., Conkright, M. E., OBrien, T. D., Stephens, C., 1998b. World ocean atlas 1998 volume 2: Temperature of the pacific ocean. NOAA Atlas NESDIS 28. US Government Printing Office: Washington, DC.

Antonov, J. I., Levitus, S., Boyer, T. P., Conkright, M. E., OBrien, T. D., Stephens, C., 1998c. World ocean atlas 1998 volume 3: Temperature of the indian ocean. NOAA Atlas NESDIS 29. US Government Printing Office: Washington, DC.

Antonov, J. I., Locarnini, R. A., Boyer, T. P., Mishonov, A. V., Garcia, H. E., 2006. World ocean atlas 2005, volume 2: Salinity, s. levitus (ed.). NOAA Atlas NESDIS 62. US Government Printing Office: Washington, DC.

Balgovind, R., Dalcher, A., Ghil, M., Kalnay, E., 1983. A stochasticdynamic model for the spatial structure of forecast error statistics. Monthly Weather Review 111, 701–722.

Barnes, S. L., 1964. A technique for maximizing details in numerical weather map analysis. Journal of Applied Meteorology 3, 396–409.

Barnes, S. L., 1973. Mesoscale objective map analysis using weighted time series observations. NOAA Technical Memorandum ERL NSSL-62.

Barnes, S. L., 1994. Applications of the barnes objective analysis scheme, part iii: Tuning for minimum error. Journal of Atmospheric and Oceanic Technology 11, 1459–1479.

Bertsimas, D., Tsitsiklis, J. N., 1997. Introduction to Linear Optimization. Athena Scientific, Belmont, Massachusetts.

Boyer, T. P., Levitus, S., Antonov, J. I., Conkright, M. E., OBrien, T. D., Stephens, C., 1998a. World ocean atlas 1998 volume 1: Temperature of the atlantic ocean. NOAA Atlas NESDIS 30. US Government Printing Office: Washington, DC.

Boyer, T. P., Levitus, S., Antonov, J. I., Conkright, M. E., OBrien, T. D., Stephens, C., 1998b. World ocean atlas 1998 volume 2: Temperature of the pacific ocean. NOAA Atlas NESDIS 31. US Government Printing Office: Washington, DC.

Boyer, T. P., Levitus, S., Antonov, J. I., Conkright, M. E., OBrien, T. D., Stephens, C., 1998c. World ocean atlas 1998 volume 3: Temperature of the indian ocean. NOAA Atlas NESDIS 32. US Government Printing Office: Washington, DC.

Boyer, T. P., Stephens, C., Antonov, J. I., Conkright, M. E., Locarnini, R. A., OBrien, T. D., Garcia, H. E., 2002. World ocean atlas 2001 volume 2: Salinity, s. levitus (ed.). NOAA Atlas NESDIS 50. US Government Printing Office: Washington, DC.

Bresenham, J. E., 1965. Algorithm for computer control of a digital plotter. IBM Systems Journal 4 (1), 25–30.

Bretherton, F. P., Davis, R. E., Fandry, C., 1976. A technique for objective analysis and design of oceanographic instruments applied to mode-73. Deep-Sea Research 23, 559–582.

Brown, R. G., Hwang, P. Y. C., 1997. Introduction to Random Signals and Applied Kalman Filtering. John Wiley & Sons, United Kingdom.

Burton, L., 2009. Modeling coupled physics and biology in ocean straits. SM Thesis, Massachusetts Institute of Technology.

Carter, E., Robinson, A., 1987. Analysis models for the estimation of oceanic fields. Journal of Atmospheric and Oceanic Technology 4 (1), 49–74.

Cho, Y., Shin, V., Oh, M., Lee, Y., 1996. Suboptimal continuous filtering based on the decomposition of the observation vector. Computers and Mathematics with applications 32 (4), 23–31.

Cossarini, G., Lermusiaux, P. F. J., Solidoro, C., 2009. The lagoon of venice ecosystem: Seasonal dynamics and environmental guidance with uncertainty analyses and error subspace data assimilation. Journal of Geophysical Research.

Cressman, G. P., 1959. An operational objective analysis scheme. Monthly Weather Review 87, 329–340.

Daley, R., 1993. Atmospheric Data Analysis. Cambridge University Press.

Denman, K. L., Freeland, H. J., 1985. Correlation scales, objective mapping and a statistical test of geostrophy over the continental shelf. Journal of Marine Research 43, 517–539.

Dolloff, J., Lofy, B., Sussman, A., Taylor, C., 2006. Strictly positive definite correlation functions. Proceedings of SPIE 6235.

Gamo, T., Kato, Y., Hasumoto, H., Kakiuchi, H., Momoshima, N., Takahata, N., Sano, Y., 2007. Geochemical implications for the mechanism of deep convection in a semi-closed tropical marginal basin: Sulu sea. Deep-Sea Research II 54, 4–13.

Gandin, L. S., 1965. Objective analysis of meteorological fields. Israel Program for Scientific Translations.

Garcia, H. E., Locarnini, R. A., Boyer, T. P., Antonov, J. I., 2006a. World ocean atlas 2005, volume 3: Dissolved oxygen, apparent oxygen utilization, and oxygen saturation, s. levitus (ed.). NOAA Atlas NESDIS 63. US Government Printing Office: Washington, DC.

Garcia, H. E., Locarnini, R. A., Boyer, T. P., Antonov, J. I., 2006b. World ocean atlas 2005, volume 4: Nutrients (phosphate, nitrate, silicate), s. levitus (ed.). NOAA Atlas NESDIS 64. US Government Printing Office: Washington, DC.

Gordon, A. L., 2009. Philex: Regional cruise intensive observational period, leg 1 and 2 reports.

Haley, P. J., Lermusiaux, P. F. J., Agarwal, A., 2009. Minimizing the inter-island transport using an optimization methodology. Submitted to Ocean Modelling.

Haley, P. J., Lermusiaux, P. F. J., Robinson, A. R., Leslie, W. G., Logoutov, O. G., Cossarini, G., Liang, X. S., Moreno, P., Ramp, S. R., Doyle, J. D., Bellingham, J., Chavez, F., Johnston, S., 2008. Forecasting and reanalysis in the monterey bay/california current region for the autonomous ocean sampling network-ii experiment. Deep Sea Research II.

Hessler, G., 1984. Experiments with statistical objective analysis techniques for representing a coastal surface temperature field. Boundary Layer Meteorology 28, 375–389.

Lermusiaux, P. F. J., 1997. Error subspace data assimilation methods for ocean field estimation: Theory, validation and applications. PhD Thesis, Harvard University.

Lermusiaux, P. F. J., July 1999. Data assimilation via error subspace statistical estimation. part ii: Middle atlantic bight shelfbreak front simulations and esse validation. Monthly Weather Review 127, 1408–1432.

Lermusiaux, P. F. J., 2002. On the mapping of multivariate geophysical fields: Sensitivities to size, scales, and dynamics. Journal of Atmospheric and Oceanic Technology 19, 1602–1637.

Lermusiaux, P. F. J., 2007. Adaptive modeling, adaptive data assimilation and adaptive sampling. Physica D 230, 172–196.

Lermusiaux, P. F. J., Anderson, D. G. M., Lozano, C. J., 2000. On the mapping of multivariate geophysical fields: Error and variability subspace estimates. Quarterly Journal of the Royal Meteorological Society 126, 1387–1429.

Lermusiaux, P. F. J., Lozano, C. J., Anderson, D. G., 1998. On the mapping of multivariate geophysical fields: studies of the sensitivity to error subspace parameters. Harvard Open Ocean Model Report No. 58, Harvard University.

Lermusiaux, P. F. J., Robinson, A. R., July 1999. Data assimilation via error subspace statistical estimation. part i: Theory and schemes. Monthly Weather Review 127, 1385–1407.

Levitus, S., 1982. Climatological atlas of the world ocean. NOAA Professional Paper 13. US. Government Printing Office: Washington,DC.

Levitus, S., Boyer, T. P., 1994. World ocean atlas 1994: Volume 4: Temperature. NOAA Atlas NESDIS 4. US Government Printing Office: Washington, DC.

Levitus, S., Burgett, R., Boyer, T. P., 1994. World ocean atlas 1994, volume 3: Salinity. NOAA Atlas NESDIS 3. US Government Printing Office: Washington, DC.

Locarnini, R. A., Mishonov, A. V., Antonov, J. I., Boyer, T. P., Garcia, H. E., 2006. World ocean atlas 2005, volume 1: Temperature, s. levitus (ed.). NOAA Atlas NESDIS 61, U.S. Government Printing Office: Washington, D.C.

Logoutov, O. G., 2008. A multigrid methodology for assimilation of measurements into regional tidal models. Ocean Dynamics 58, 441–460.

Lynch, D. R., McGillicuddy, D. J., January 2001. Objective analysis for coastal regimes. Continental Shelf Research 21, 1299–1315.

Osher, S., Sethian, J. A., 1988. Fronts propagating with curvature-dependent speed: algorithms based on hamilton-jacobi formulations. Journal of Computational Physics 79 (1), 12–49.

Papoulis, A., 1991. Probability, Random Variables and Stochastic Processes. McGraw-Hill.

Paris, C. B., Cowen, R. K., Lwiza, K. M. M., Wang, D. P., Olson, D. B., 2002. Multivariate objective analysis of the coastal circulation of barbados, west indies: implication for larval transport. Deep-Sea Research I 49, 1363–1386.

Parrish, D. F., Cohn, S. E., 1985. A kalman filter for a two-dimensional shallow-water model: Formulation and preliminary experiments. Office Note 304, U.S. Department of Commerce, NOAA, NWS, NMC.

Pedlosky, J., 1987. Geophysical Fluid Dynamics. Springer.

Plackett, R. L., 1950. Some theorems in least squares. Biometrika 37 (1-2), 149–157.

Ruoy, E., Tourin, A., 1992. A viscosity solutions approach to shape from shading. SIAM Journal on Numerical Analysis 29, 867–884.

Sedgewick, R., 1988. Algorithms. Addison-Wesley.

Selvadurai, A. P. S., 2000. Partial Differential Equations in Mechanics. Springer.

Sethian, J. A., 1996. A fast marching level set method for monotonically advancing fronts. Proceedings of the National Academy of Sciences 93 (4), 1591–1595.

Sethian, J. A., 1999a. Fast marching methods. SIAM Review 41 (2), 199–235.

Sethian, J. A., 1999b. Level Set Methods and Fast Marching Method. Cambridge University Press, Cambridge, United Kingdom.

Stacey, M. W., Pond, S., LeBlond, P. H., 1988. An objective analysis of the low-frequency currents in the strait of georgia. Atmosphere-Ocean 26 (1), 1–15.

Stephens, C., Antonov, J. I., Boyer, T. P., Conkright, M. E., Locarnini, R. A., OBrien, T. D., Garcia, H. E., 2002. World ocean atlas 2001 volume 1: Temperature, s. levitus (ed.). NOAA Atlas NESDIS 49. US Government Printing Office: Washington, DC.

Williams, J. W. J., 1964. Algorithm 232 - heapsort. Communications of the ACM 7 (6), 347348.

Wunsch, C., 1996. The Ocean Circulation Inverse Problem. Cambridge University Press, Cambridge, United Kingdom.

Xu, J., Lermusiaux, P. F. J., Haley, P. J., Leslie, W. G., Logoutov, O. G., 2008. Spatial and temporal variations in acoustic propagation during the plusnet07 exercise in dabob bay. Proceedings of Meetings on Acoustics (POMA), 155th Meeting Acoustical Society of America 4.

Yaglom, A. M., 1987. Correlation theory of stationary and related random functions I. Springer-Verlag.

Yaglom, A. M., 2004. An Introduction to the Theory of Stationary Random Functions (Dover Phoenix Editions). Dover.

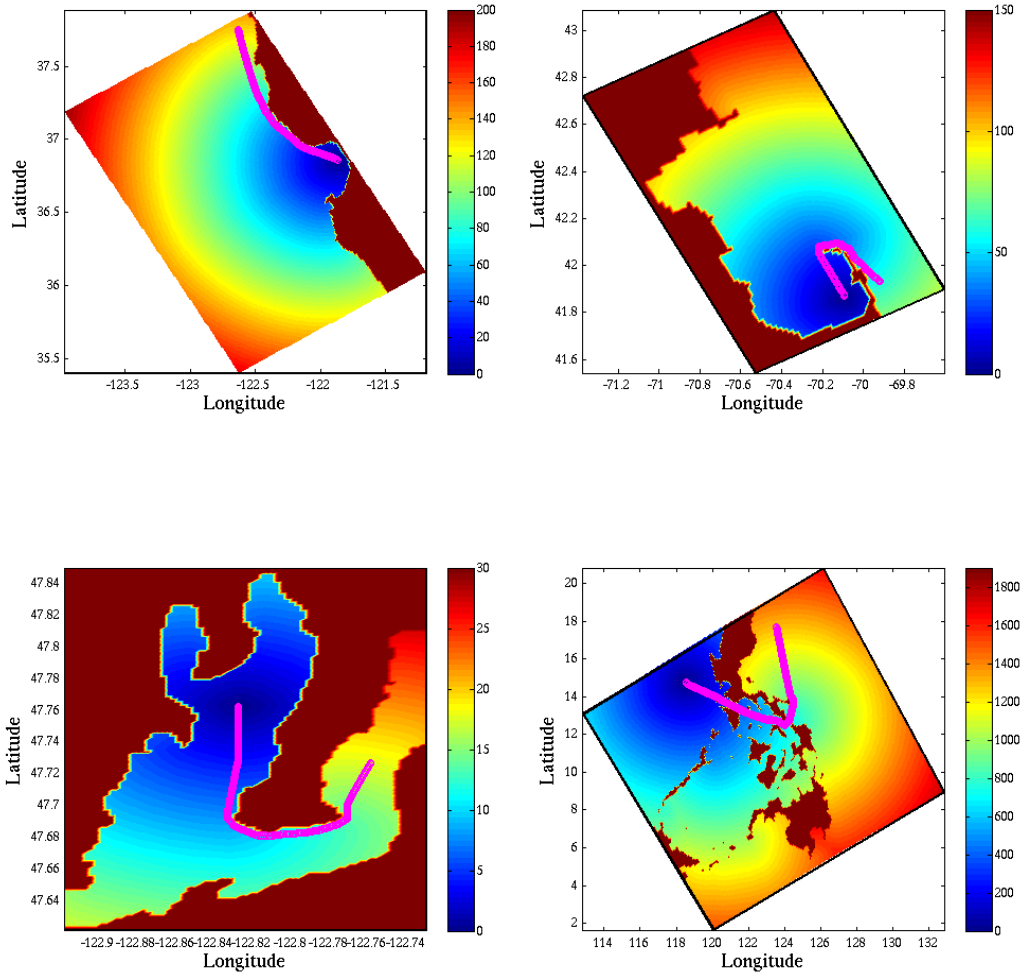

Figure 1: Optimal distances and path in: (Top - Left) Monterey Bay; (Top - Right) Massachusetts Bay; (Bottom - Left) Dabob Bay; (Bottom - Right) Philippines Archipelago.

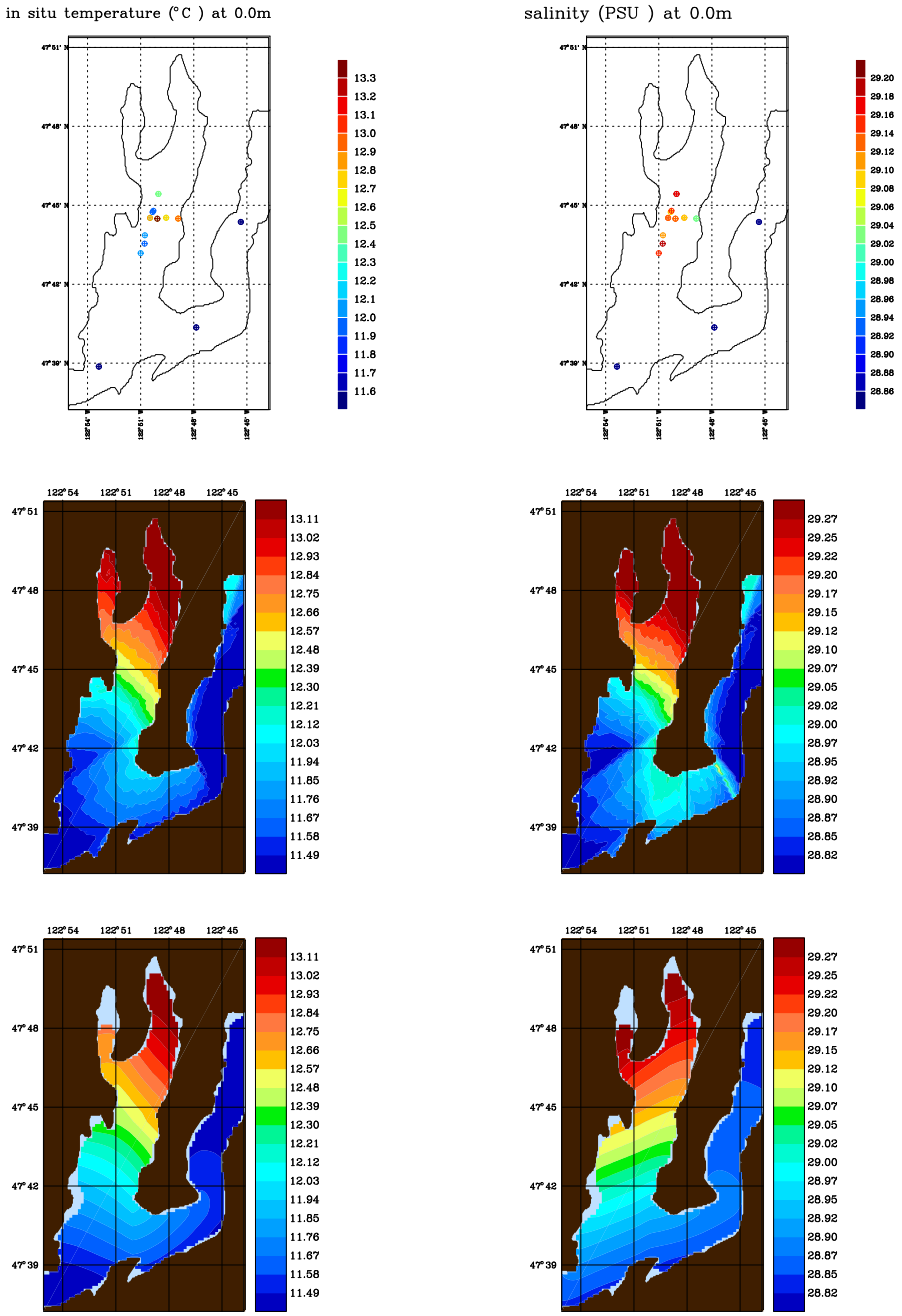

Figure 2: Temperature (^{o}C) (Top - Left) and Salinity (PSU) (Top-Right) data in Dabob Bay; Temperature (^{o}C) (Left) and Salinity (PSU) (Right) OA Fields in Dabob Bay from the optimal path length computed using: (Middle) Bresenham-based line Algorithm; (Bottom) Fast Marching Method.

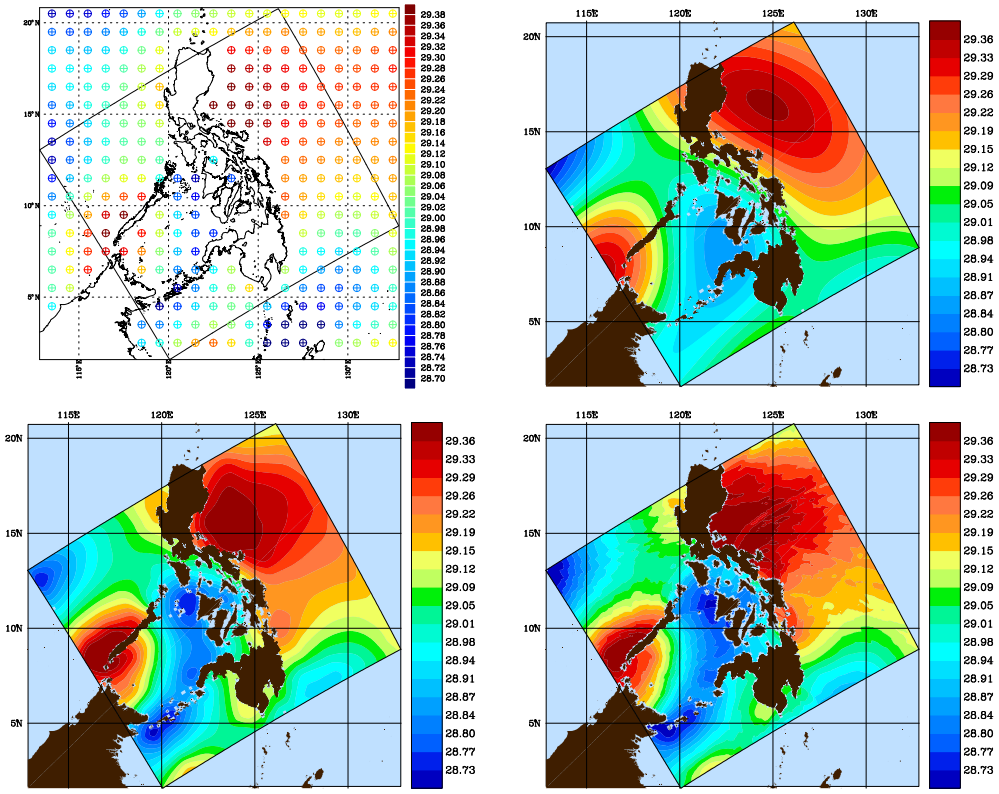

Figure 3: (Top - Left) World Ocean Atlas 2005 Climatology in situ temperature (^{o}C) at 0m; Temperature (^{o}C) OA Fields obtained using: (Top - Right) Standard OA without taking islands into account; (Bottom - Left) Fast Marching Method; (Bottom - Right) SPDE approach (representing field by a stochastically forced Helmholtz Equation).

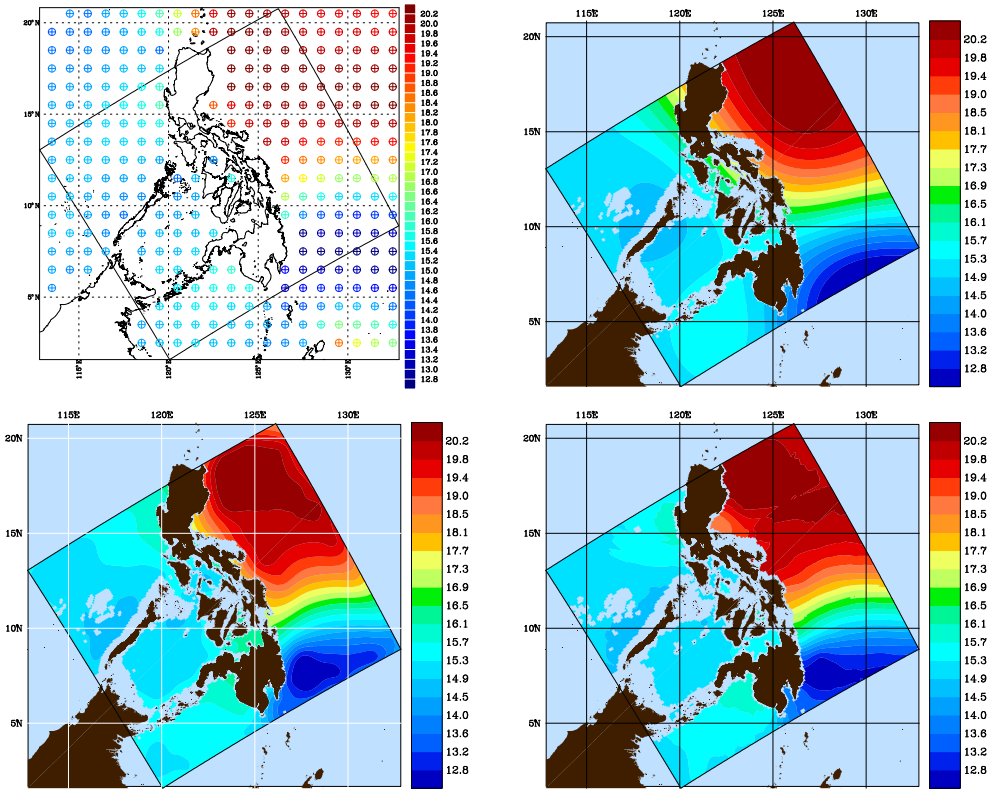

Figure 4: (Top - Left) World Ocean Atlas 2005 Climatology in situ temperature (^{o}C) at 200.0m; Temperature (^{o}C) OA Fields obtained using: (Top - Right) Standard OA without taking islands into account; (Bottom - Left) Fast Marching Method; (Bottom - Right) SPDE approach (representing field by a stochastically forced Helmholtz Equation).

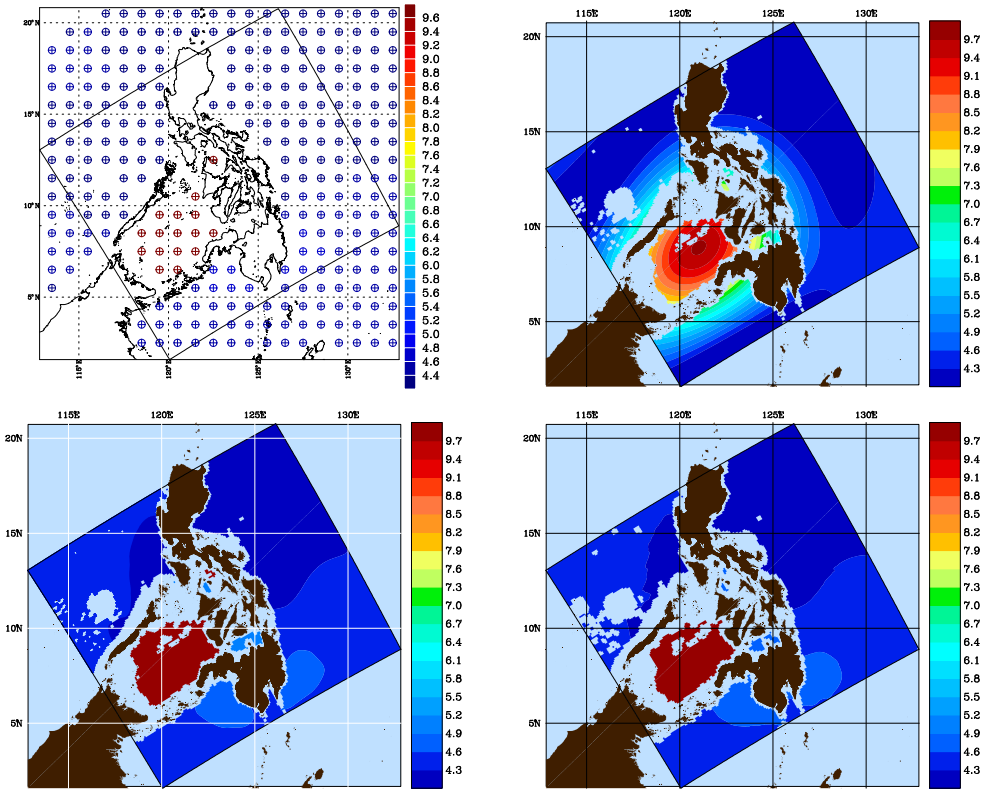

Figure 5: (Top - Left) World Ocean Atlas 2005 Climatology in situ temperature (^{o}C) at 1000.0m; Temperature (^{o}C) OA Fields obtained using: (Top - Right) Standard OA without taking islands into account; (Bottom - Left) Fast Marching Method; (Bottom - Right) SPDE approach (representing field by a stochastically forced Helmholtz Equation).

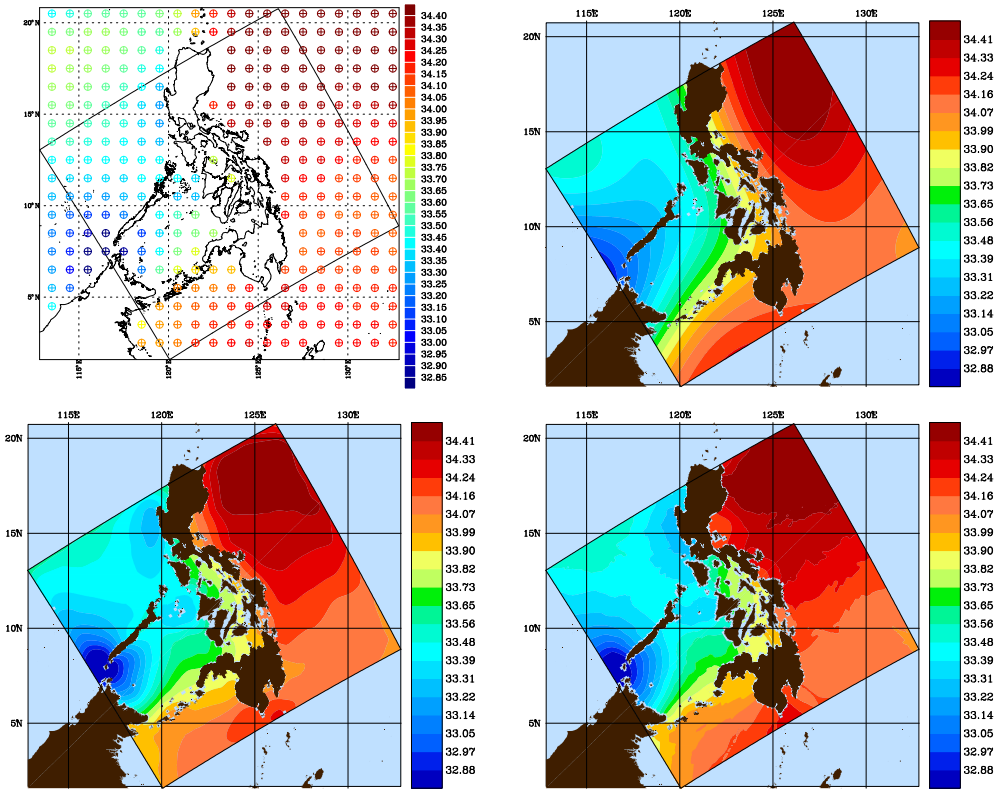

Figure 6: (Top - Left) World Ocean Atlas 2005 Climatology in situ Salinity (PSU) at 0m; Salinity (PSU) OA Fields obtained using: (Top - Right) Standard OA without taking islands into account; (Bottom - Left) Fast Marching Method; (Bottom - Right) SPDE approach (representing field by a stochastically forced Helmholtz Equation).

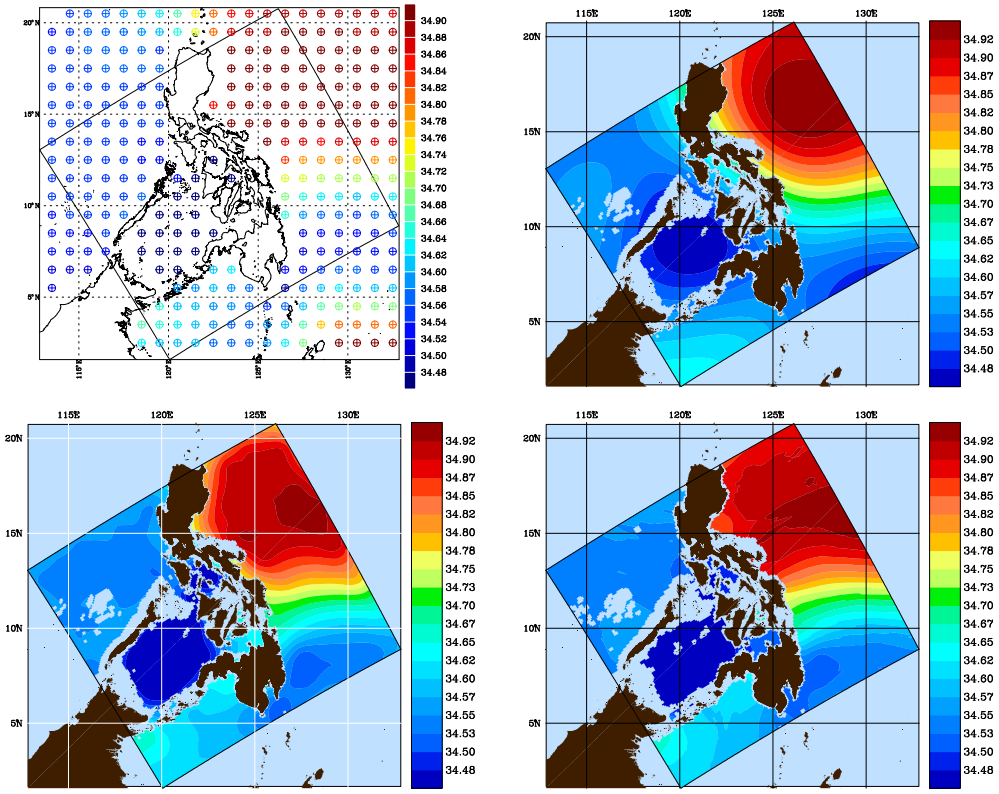

Figure 7: (Top - Left) World Ocean Atlas 2005 Climatology in situ Salinity (PSU) at 200.0m; Salinity (PSU) OA Fields obtained using: (Top - Right) Standard OA without taking islands into account; (Bottom - Left) Fast Marching Method; (Bottom - Right) SPDE approach (representing field by a stochastically forced Helmholtz Equation).

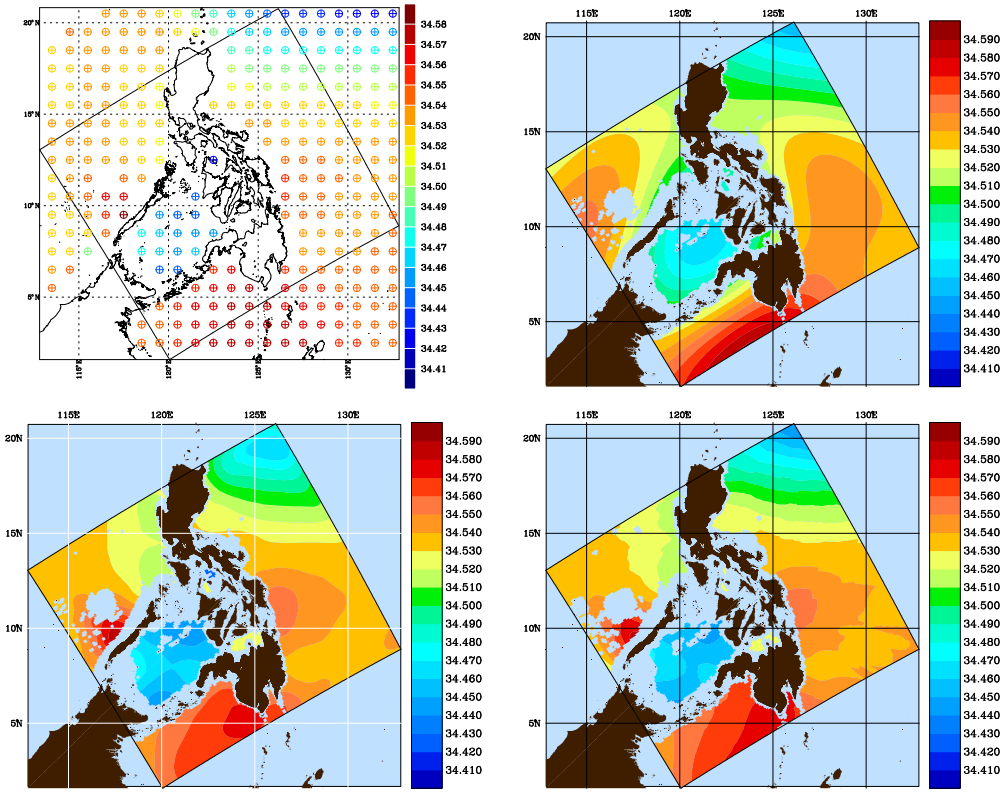

Figure 8: (Top - Left) World Ocean Atlas 2005 Climatology in situ Salinity (PSU) at 1000.0m; Salinity (PSU) OA Fields obtained using: (Top - Right) Standard OA without taking islands into account; (Bottom - Left) Fast Marching Method; (Bottom - Right) SPDE approach (representing field by a stochastically forced Helmholtz Equation).

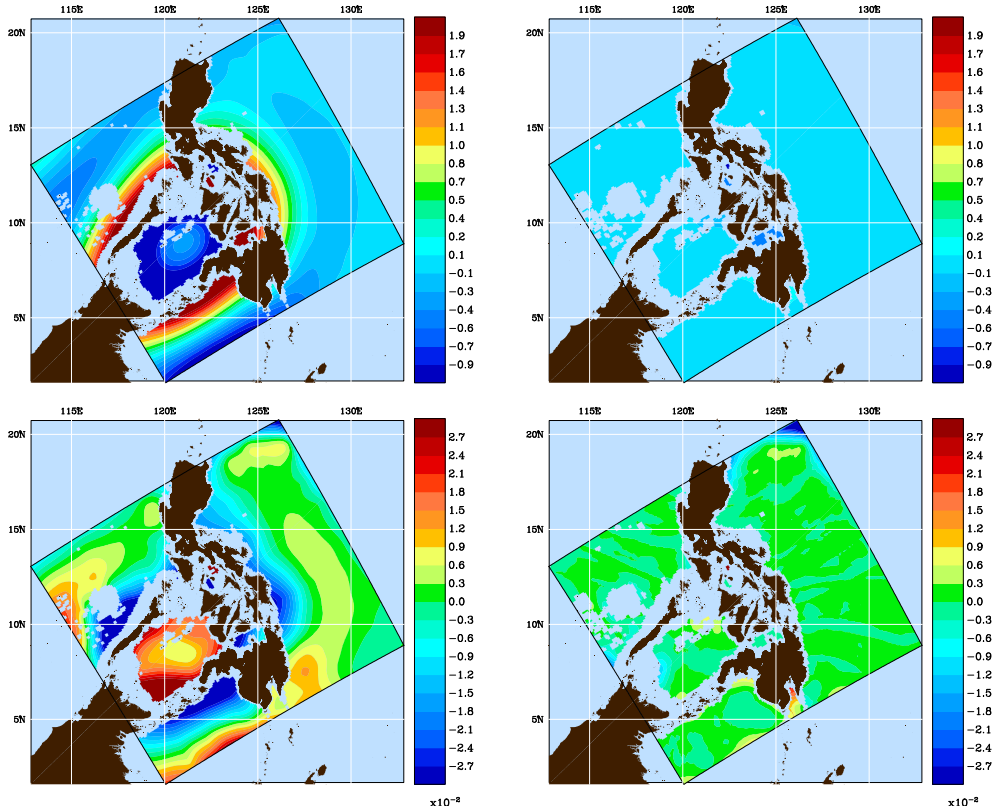

Figure 9: Difference between Temperature (^{o}C) field at Level = 1000m obtained using Fast Marching Method and using: (Top - Left) Standard OA; (Top - Right) SPDE (representing field by Helmholtz equation). Difference between Salinity (PSU) field at Level = 1000m obtained using Fast Marching Method and using: (Bottom - Left) Standard OA; (Bottom - Right) SPDE (representing field by Helmholtz equation).

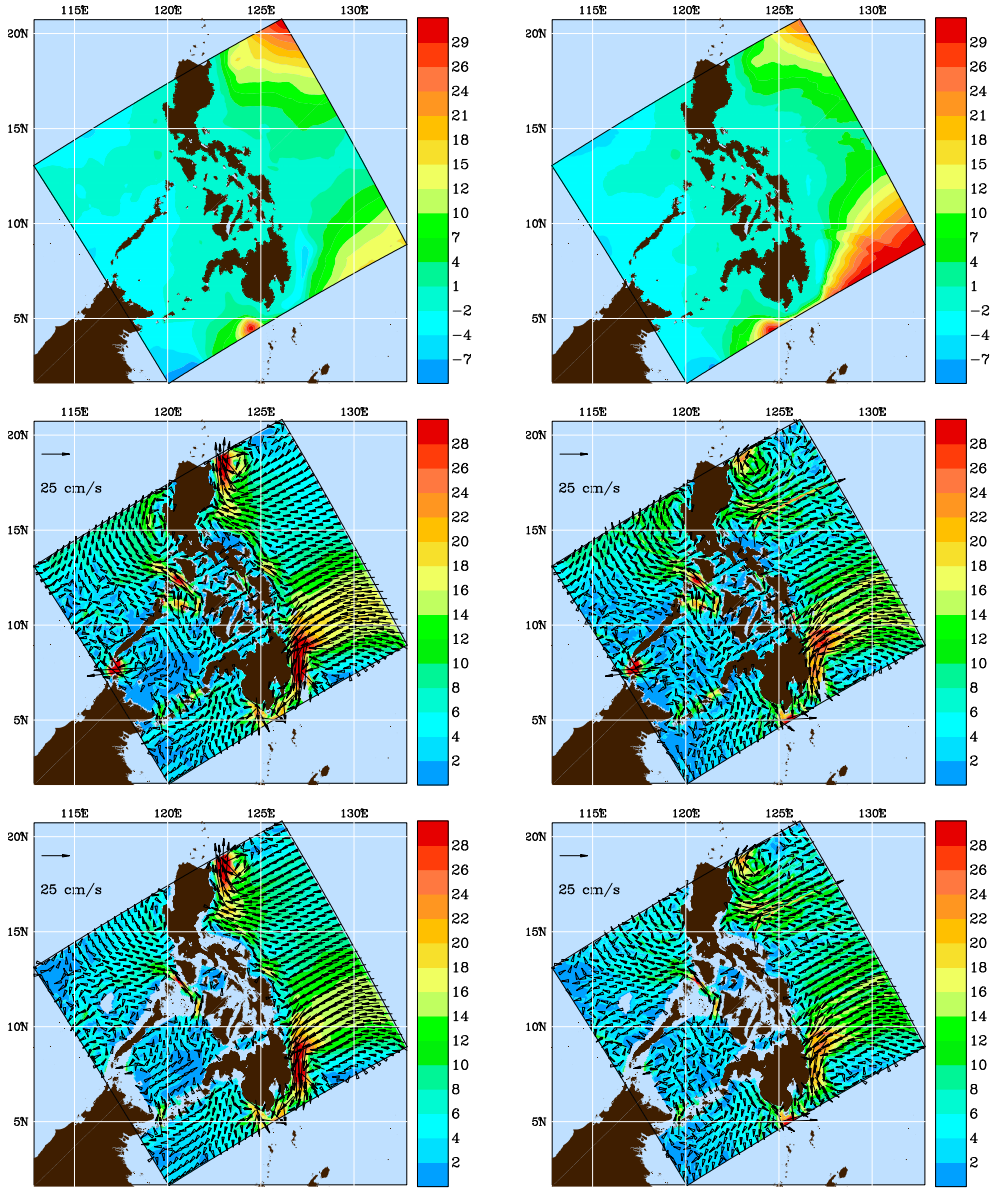

Figure 10: Velocity estimation under geostrophic balance (weight functions based on the minimum vertical area) from field maps (WOA05) obtained using the FMM (Left) and using the SPDE Approach (Right): (Top) Streamfunction, Velocity at depths: (Middle) 0m; (Bottom) 100m.

Summer 2007

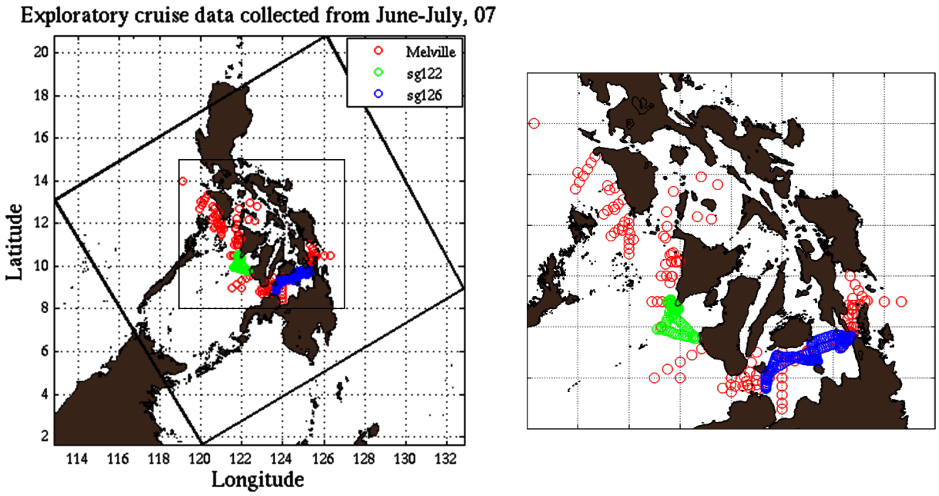

Winter 2008

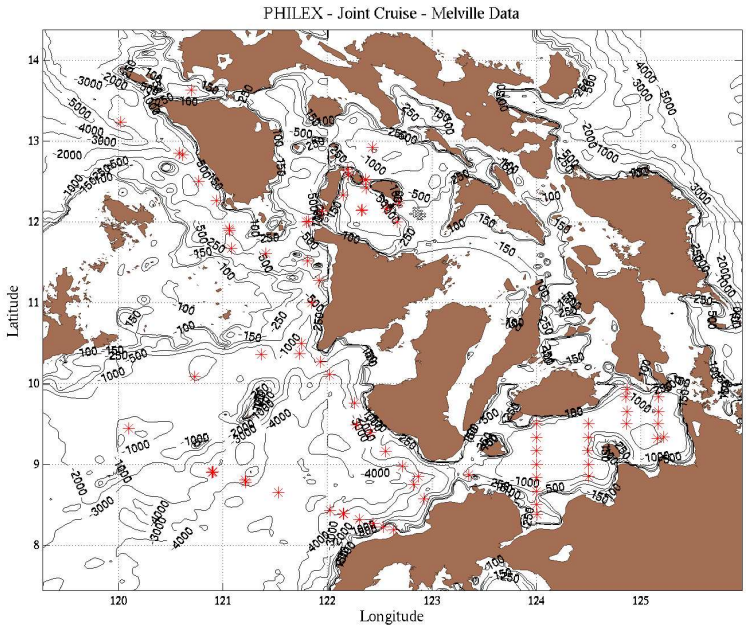

Figure 11: (Top) Melville exploratory cruise and glider data (Summer 2007) in Philippines Archipelago; (Bottom) Philippines Archipelago - Melville joint cruise Data (Winter 2008).

Summer 2007

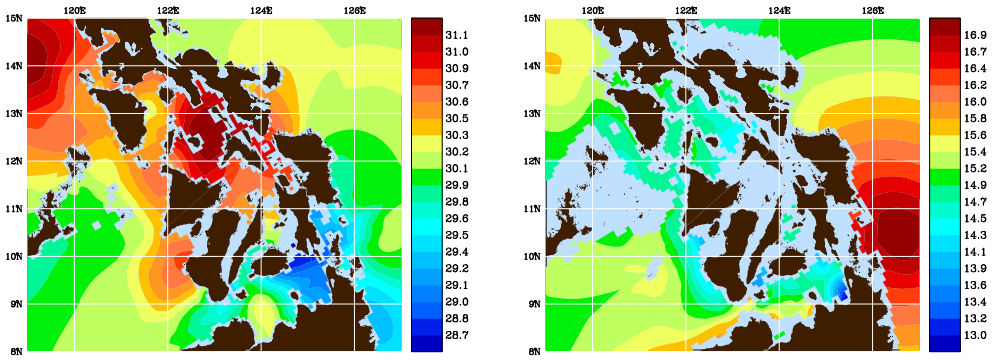

Winter 2008

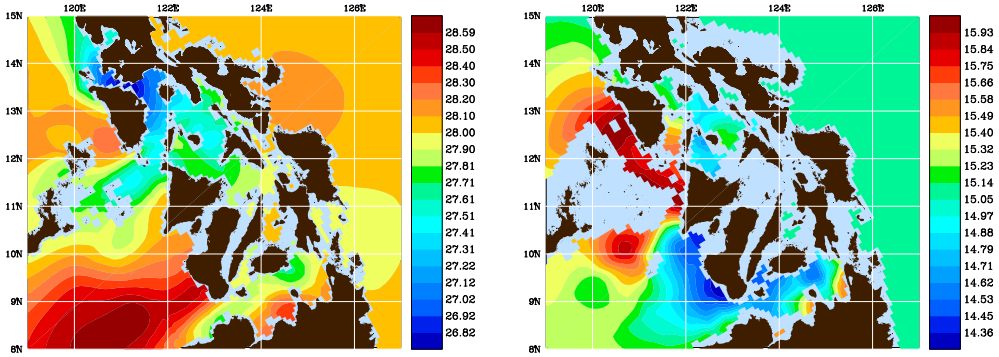

Figure 12: Temperature (^{o}C) OA Fields at 0m (Left) and 200m (Right) using the: (Top) Melville exploratory cruise and glider data (Summer 2007); (Bottom) Melville joint cruise data (Winter 2008).

Summer 2007

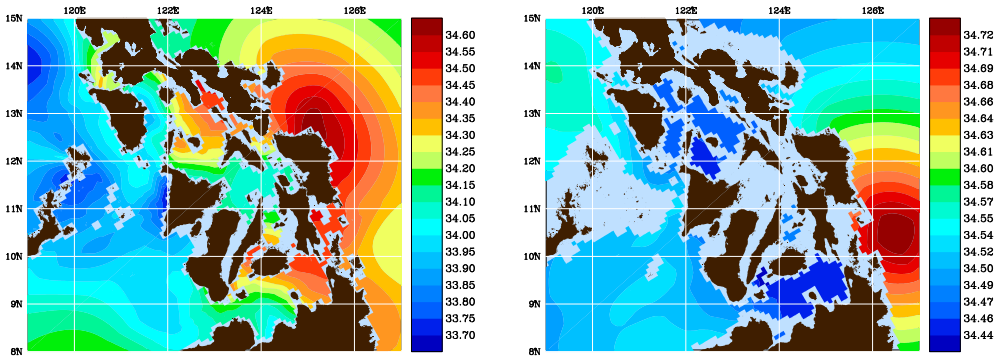

Winter 2008

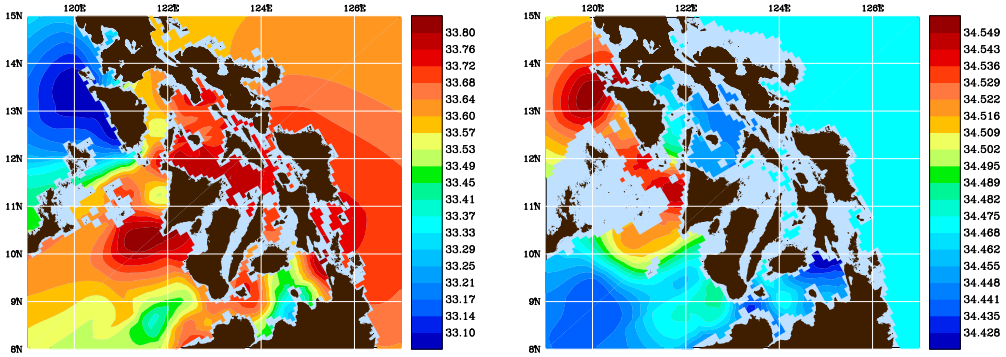

Figure 13: Salinity (PSU) OA Fields at 0m (Left) and 200m (Right) using the: (Top) Melville exploratory cruise and glider data (Summer 2007); (Bottom) Melville joint cruise data (Winter 2008).

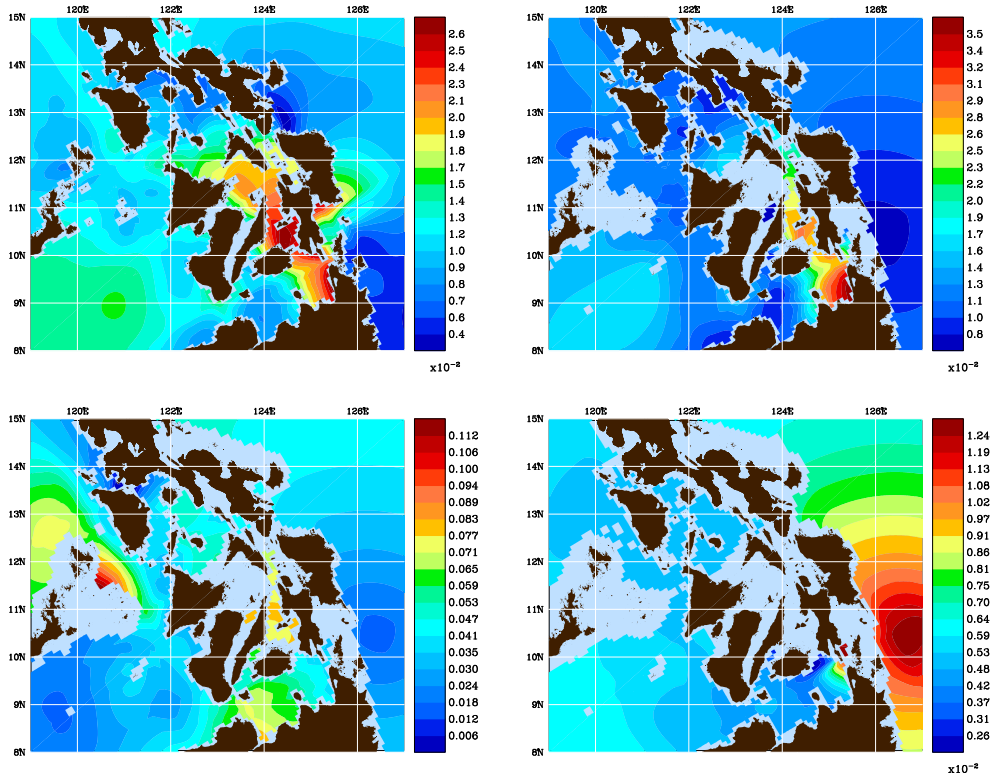

Figure 14: Chlorophyll (μmol/Kg) OA Fields using the FMM at Level: (Top - Left) 0m; (Top - Right) 10m; (Bottom - Left) 50m; (Bottom - Right) 160m.

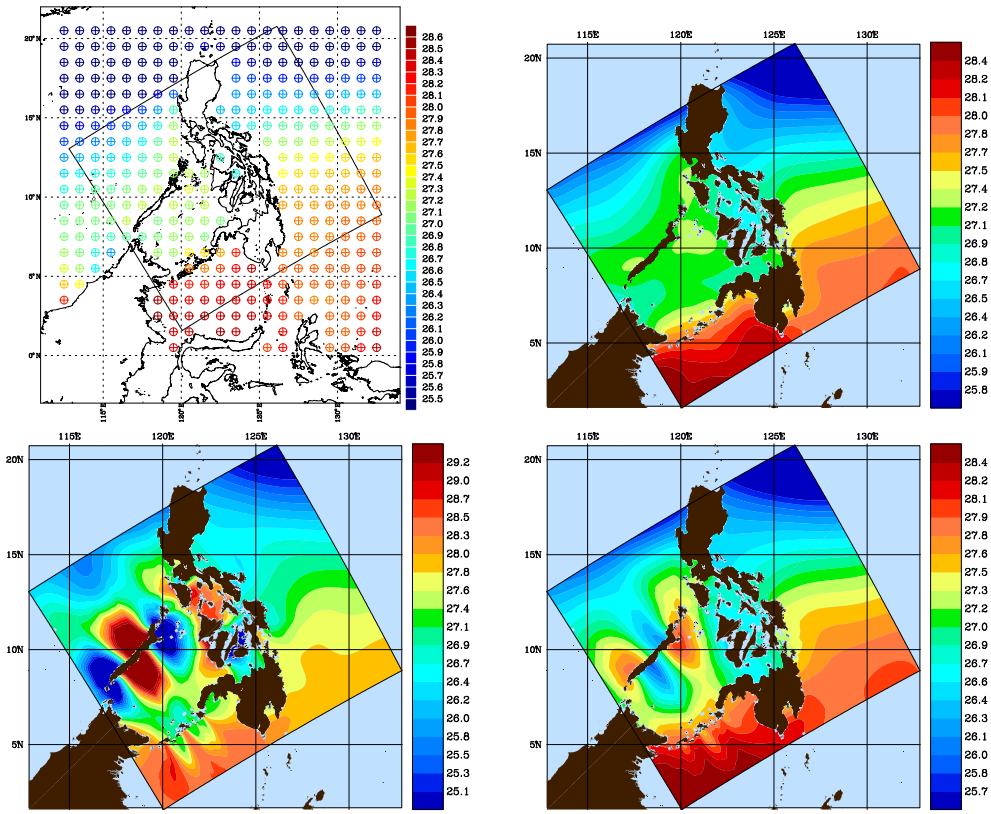

Figure 15: (Top - Left) World Ocean Atlas 2005 (Spliced February and Winter Climatology) in situ temperature (^{o}C) at 0.0m; Temperature (^{o}C) OA Fields using the Fast Marching Method at the surface (0m) using the following scheme and scales: (Top - Right) First order FMM and $L_0 = 540Km$, $L_e = 180Km$; (Bottom - Left) First order FMM and $L_0 = 1080Km$, $L_e = 360Km$; (Bottom - Right) Higher order FMM and $L_0 = 1080Km$, $L_e = 360Km$.

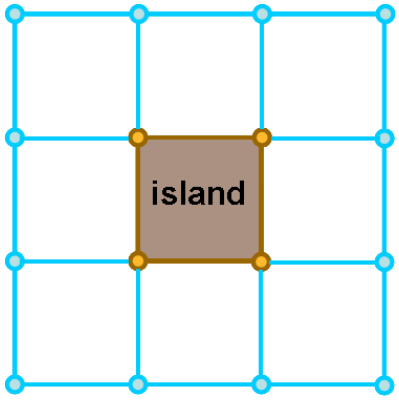

Figure 16: Example of an idealized (multiply-connected) domain having an island.

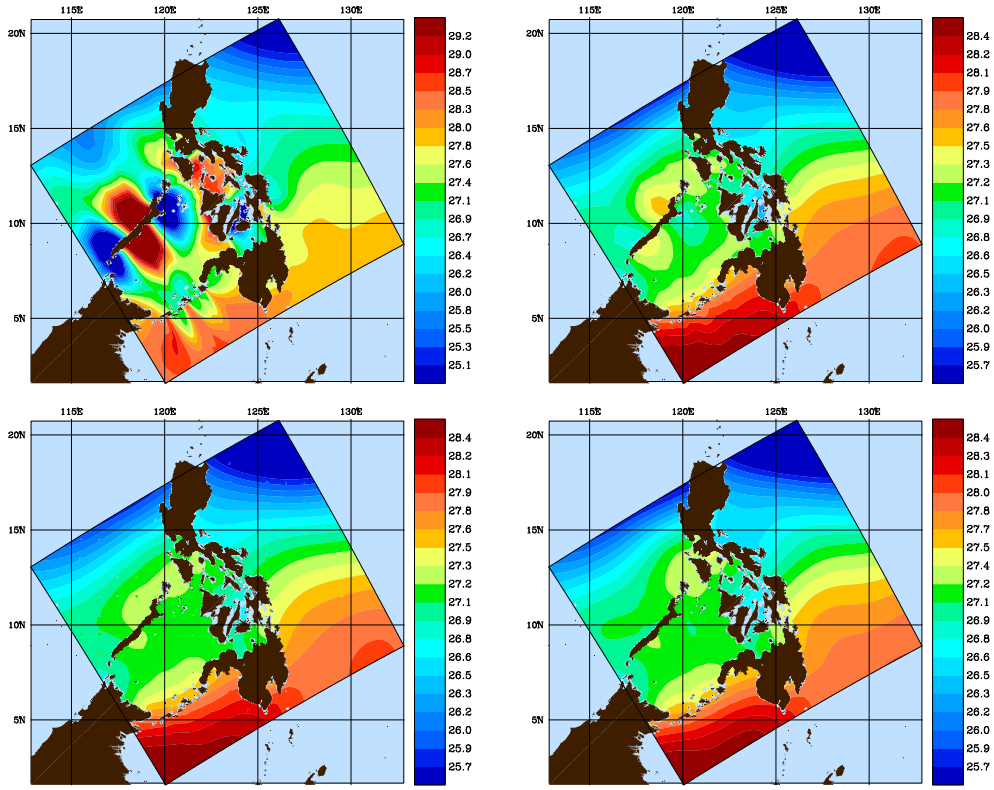

Figure 17: Temperature (^{o}C) OA Fields at the surface (0m) (scales $L_0 = 1080Km$, $L_e = 360Km$) using the : (Top - Left) FMM; (Top - Right) FMM and removal of problematic data; (Bottom - Left) FMM and introducing process noise; (Bottom - Right) FMM and applying dominant singular value decomposition (SVD) of a-priori covariance.